Meson dynamics in the $SU_3 \times SU_3$ σ model

Lai-Him Chan and Richard W. Haymaker*

Department of Physics and Astronomy, Louisiana State University, Baton Rouge, Louisiana 70803

(Received 15 July 1974)

We present the calculation of phase shifts for the renormalizable SU_3 σ model with the symmetry-breaking term $\mathcal{L}_{SB} = -\epsilon_0\sigma_0 - \epsilon_8\sigma_8$. Perturbation theory is carried out to the one-loop approximation and phase shifts are obtained from Padé approximants. We renormalize at physical quantities: masses of π, K, η, η', decay constant f_π, and the $\pi\pi$, $I = 0$, $l = 0$ S-wave scattering amplitude near threshold. As a consequence of this choice, perturbation theory is a power series in $1/f_\pi^2$. A further consequence is that there are low-energy off-mass-shell points where the tree approximation is exact, as we show. The symmetry-breaking picture is that of a nearly $SU_2 \times SU_2$-invariant Hamiltonian and a nearly SU_3-invariant vacuum. The $SU_3 \times SU_3$ limit is the Goldstone type. The corrections to decay constants and symmetry-breaking parameters are small. We can account for the size of corrections to all quantities of interest in a simple way. We achieve consistency between two measures of SU_3-symmetry breaking, i.e., m_K/m_π and f_K/f_π. That is, we find $f_K/f_\pi f_+(0) = 1.34$. With the physical value of $f_\pi (= 0.095$ GeV), and with one free parameter, m_σ(tree), we achieve qualitative agreement with experiment for the S-wave nonexotic phase shifts, and the P- and D-wave octet central masses. The exotic S-wave phase shifts are too strongly repulsive and an SU_3 $\underline{27}$ representation of states occurs in the D wave. SU_3 is a good symmetry for the P- and D-wave states in spite of large differences in the thresholds of channels generating them. The magnitude of splitting is quantitatively correct. A novel expression for the unequal-mass box graph is presented.

I. INTRODUCTION

The SU_2 and SU_3 σ models have provided valuable insight into the consequences of the postulates of current algebra and partial conservation of axial-vector current (PCAC).[1,2] There have been a number of papers in which these models have been studied in their own right as candidates for providing some unity to low-energy dynamics beyond the current-algebra predictions.[3,4] In this paper we further pursue this point of view by calculating meson-meson scattering phase shifts in the SU_3 version of the model. We calculate amplitudes in standard perturbation theory to the one-closed-loop order and employ Padé approximants to unitarize them. We use the most general form of the model with the restrictions that the interactions are renormalizable and with symmetry breaking linear in the scalar fields.

Some of the groundwork has been laid out in previous papers. In Ref. 5 we carried out the renormalization of the model in the presence of symmetry breaking. We verified that all divergences can be grouped into the renormalization of the parameters of the $SU_3 \times SU_3$-invariant part of the Lagrangian. Such is the case for the SU_2 σ model as shown by Lee[6] and Symanzik.[7] This feature is important for the course of this work and strongly prejudices us against adding further symmetry-breaking terms to the Lagrangian. Symmetry breaking that is higher order in the fields will generate divergences that cannot be grouped into existing terms in the symmetric Lagrangian and also introduce new parameters in higher order. This would in turn obscure the role of chiral symmetry in the model and possibly increase the number of parameters to an unmanageable number. In Ref. 8 (referred to as paper I) we calculated the one- and two-point functions in the one-loop approximation and fit them to decay constants and masses. In the tree approximation the picture of symmetry breaking that emerges is essentially that of Gell-Mann, Oakes, and Renner,[9] i.e., that the Hamiltonian is nearly $SU_2 \times SU_2$-symmetric, whereas the vacuum is closer to SU_3-symmetric. We found in paper I that this picture remained intact through second order in perturbation theory. The corrections to symmetry-breaking parameters, masses, and decay constants were quite small.

This paper greatly expands the scope of our earlier paper (I). Phase shifts have been calculated for all two-body channels involving π, K, and η for $l = 0$, 1, and 2. The amplitudes were calculated in the one-loop approximation and then cast into a [1, 1] Padé approximant. Coupling between these two-body channels was taken into account through a matrix Padé formalism. With

our renormalization procedure, perturbation theory is a power series in $1/f_\pi^2$, f_π being the physical pion decay constant as we show. We calculated the K_{l3} vector form factor allowing us to compare with the experimental value of $f_K/f_\pi f_+(0)$. The renormalization procedure was modified slightly from that of Ref. 8 by introducing a chiral-invariant wave-function renormalization constant. This has no effect on the determination of physical quantities but is useful for studying symmetry limits. We examine the SU_3 limit in order to ascertain the SU_3 representation content of resonances. The $SU_3 \times SU_3$ limit is of the Goldstone type. This differs from paper I, where the type of limit was ambiguous. A full analysis of this limit will be delayed to a later paper. The calculations were extensively checked. The checks included unitarity of the amplitude, the verification of Adler zeros,[10] and other low-energy theorems as will be described below.

An important effect that shows up prominently in this model is strong cancellations among classes of diagrams. This effect can be seen most easily in the tree graphs for π-π scattering, for example. For $m_\sigma^2 \to \infty$, f_π, m_π, s, and t fixed, individual graphs diverge yet the sum approaches a finite limit, as is well known. For s near the π-π threshold there are cancellations between terms of order $m_\sigma^2/4m_\pi^2$. The cancellations are quite a general feature and arise because the low-energy region is essentially fixed by the Ward identities arising from chiral symmetry order by order in perturbation theory but not graph by graph. We also note that in second order, for example, the discontinuities across pseudoscalar cuts contain products of tree graphs. The cancellations were in some cases as large as a factor of 10^5, making roundoff error a knotty problem.

This effect can account for several discrepancies between our determination of parameters in this paper and our determination in the earlier paper I. Notably we find an improved f_K/f_π (≈ 1.31 as compared to 1.45 in paper I). This will be discussed below, but suffice it to say that this difference can be traced to a shortcoming in our treatment of the scalar mesons in paper I. In paper I we determined their masses and widths from two-point function graphs, and in this paper from scattering graphs. The former did not have the cancellations that the latter exhibit. Although this distinction would make no difference in exact solutions, it is quite important in low orders.

To what extent should we expect perturbation theory through the one-loop order to give reliable solutions to this field theory? There are a number of quantities that are probably determined very well in this approximation. These include decay constants, wave-function renormalization constants, and symmetry-breaking parameters, all of which have small corrections. We show that these are low-energy points for π-π scattering amplitudes where the tree approximation is exact for our choice of renormalization subtraction points. Hence the low-energy region of scattering amplitudes is also very well determined. For higher energies, i.e., the region where we look for dynamically generated states, 800 to 1600 MeV, the approximation is certainly much less reliable. The second-order part must be the order of magnitude of the tree order in order to generate these states. Without going to next order, the convergence of the Padé approximants is always in question despite some impressive convergence studies.[11] We feel that the spectrum generated in the P and D waves gives an indication of the strength of the forces in the various channels.

The paper is organized as follows. Section II reviews the Lagrangian and the fit of parameters at the tree level. Section III establishes some of the low-energy theorems applicable to our calculation. In Sec. IV we express the scattering tree graphs in terms of masses and decay constants in order to exhibit the low-energy theorems and the cancellation between graphs mentioned above. We further estimate the relative force strengths from these graphs. The second-order calculation is described in Sec. V, with the numerical results for the fit to experiment in Sec. VI. In Sec. VII we go to the SU_3 limit in order to ascertain the SU_3 content of the dynamically generated states. Appendix A gives a novel treatment of the box and related graphs for unequal masses. Appendixes B and C give the needed projection on angular momentum and internal symmetries.

II. LAGRANGIAN, REVIEW OF TREE SOLUTION

The basic groundwork for this paper was laid down in paper I. In this section we review the necessary steps leading up to the Feynman rules and refer the reader to paper I for more detail. There are a few minor changes that are useful for the present paper and we attempt to improve the notation.

A. Lagrangian, renormalization constants

The Lagrangian is constructed out of the fields

$$M^0 = \frac{1}{\sqrt{2}} \sum_{i=0}^{8} \lambda^i (\sigma_i^0 + i\phi_i^0), \tag{2.1}$$

where σ_i^0 and ϕ_i^0 are nonets of pseudoscalar and scalar unrenormalized fields, where M^0 belongs to the $(3, \bar{3})$ representation of $SU_3 \times SU_3$ (Ref. 12):

$$\begin{aligned}
&\mathfrak{L} = \mathfrak{L}_{\rm sym} + \mathfrak{L}_{\rm SB}\,,\\
&\mathfrak{L}_{\rm sym} = \tfrac{1}{2}\,\mathrm{Tr}(\partial_\mu M^0\,\partial^\mu M^{0\dagger}) - \tfrac{1}{2}(\mu^0)^2\,\mathrm{Tr}(M^0 M^{0\dagger})\\
&\qquad + g^0(\det M^0 + \mathrm{H.c.}) + f_1^0(\mathrm{Tr}\,M^0 M^{0\dagger})^2\\
&\qquad + f_2^0\,\mathrm{Tr}(M^0 M^{0\dagger} M^0 M^{0\dagger})\,,\\
&\mathfrak{L}_{\rm SB} = -\epsilon_0^0\sigma_0^0 - \epsilon_8^0\sigma_8^0\,.
\end{aligned} \tag{2.2}$$

The superscript 0 on parameters means bare quantities; on fields it means unrenormalized. We depart from paper I by introducing a chiral-invariant wave-function renormalization constant[13]:

$$M^0 = C^{1/2} M$$

(see Table I). In terms of the renormalized fields M, the Lagrangian can be written

$$\begin{aligned}
\mathfrak{L}_{\rm sym} = C\big[&\tfrac{1}{2}\,\mathrm{Tr}(\partial_\mu M\,\partial^\mu M^\dagger) - \tfrac{1}{2}\mu^2 Z_\mu\,\mathrm{Tr}(MM^\dagger)\\
&+ g Z_g(\det M + \mathrm{H.c.}) + f_1 Z_{f_1}(\mathrm{Tr}\,MM^\dagger)^2\\
&+ f_2 Z_{f_2}\,\mathrm{Tr}(MM^\dagger MM^\dagger)\big]\,,\\
\mathfrak{L}_{\rm SB} = -C(&\epsilon_0 Z_{\epsilon_0}\sigma_0 + \epsilon_8 Z_{\epsilon_8}\sigma_8)\,.
\end{aligned} \tag{2.3}$$

The Z_p ($p = f_1, f_2, g, \mu^2, \epsilon_0, \epsilon_8$) have been defined in such a way that C occurs as an overall factor. The following alternative expressions are given to clarify this point:

$$\begin{aligned}
&C\mu^2 Z_\mu = C(\mu^2 + \delta\mu^2) = C(\mu^0)^2\,,\\
&C g Z_g = C^{3/2}(g + \delta g) = C^{3/2} g^0\,,\\
&C f_i Z_{f_i} = C^2(f_i + \delta f_i) = C^2 f_i^0\,,\\
&C\epsilon_i Z_{\epsilon_i} = C^{1/2}(\epsilon_i + \delta\epsilon_i) = C^{1/2}\epsilon_i^0\,.
\end{aligned} \tag{2.4}$$

We define perturbation theory as an expansion in powers of λ, where

TABLE I. Summary of notations for fields and propagators. $\tilde{\Delta}$ denotes the quantity $\langle T(\sigma\sigma)\rangle$ and is not a propagator since $\langle\sigma\rangle \neq 0$. $Z_{\alpha a}$ is a wave-function renormalization constant $= \delta_{\alpha a}$ in lowest order; Z_{ia} contains the tree-order mixing angle θ_p in lowest order. We adhere to the index convention given here. The subscript T refers to states diagonalized at tree level; the subscript P to physical states. Hence the index type indicates the basis.

	Fields	Propagators
Unrenormalized	M^0	$\phi^0 : D^0_{ij}, D^0_{\alpha\beta}$
	σ_i^0, ϕ_i^0	$\sigma^0 : \tilde{\Delta}^0_{ij}, \tilde{\Delta}^0_{\alpha\beta}$
	$\sigma_\alpha^0, \phi_\alpha^0$	$S^0 : \Delta^0_{ij}, \Delta^0_{\alpha\beta}$
Chiral-invariant renormalized	M	$\phi : D_{ij}, D_{\alpha\beta}$
	σ_i, ϕ_i	$\sigma : \tilde{\Delta}_{ij}, \tilde{\Delta}_{\alpha\beta}$
	$\sigma_\alpha, \phi_\alpha$	$S : \Delta_{ij}, \Delta_{\alpha\beta}$
Fully renormalized	ϕ_a^R	$\phi_a^R : D^R_{ab}$
		$D^R_{ab}(s) \underset{s\to m_a^2}{\sim} \dfrac{\delta_{ab}}{s - m_a^2}$

Connecting relations

$(\sigma, \phi) = C^{-1/2}(\sigma^0, \phi^0)$	$\phi_a^R = Z_{\alpha a}{}^{-1/2}\phi_\alpha^0$
$\phi_i = R^\phi_{i\alpha}\phi_\alpha$	$Z_{\alpha a}{}^{-1/2} = \delta_{\alpha a} - \tfrac{1}{2}\delta Z_{\alpha a}$
$\sigma_i = R^S_{i\alpha}\sigma_\alpha$	$Z_{\alpha a}{}^{1/2} = \delta_{\alpha a} + \tfrac{1}{2}\delta Z_{\alpha a}$
	$Z_{ia}{}^{-1/2} = R^\phi_{i\alpha} Z_{\alpha a}{}^{-1/2}$

Index convention

$i, j, k, \ldots = 0, 1, \ldots, 8$		
$\alpha, \beta, \gamma, \ldots = 1, \ldots, 7$	η_T, η'_T	pseudoscalars
	σ_T, σ'_T	scalars
$a, b, c, \ldots = 1, \ldots, 7$	η_P, η'_P	pseudoscalars

$$\mathcal{L}(M,\lambda)=\frac{1}{\lambda^2}\,\mathcal{L}(\lambda M)\,, \tag{2.5}$$

and where

$$\begin{Bmatrix} C \\ Z_p \end{Bmatrix} = 1+\lambda^2\times(\text{power series in }\lambda^2)\,.$$

Lowest order in λ^2 gives tree graphs; the next order gives one-closed-loop corrections together with tree graphs arising from the explicit $\lambda^2\delta C$, and $\lambda^2\delta Z_p$. The Z_{f_1}, Z_{f_2}, Z_g, and Z_μ have infinite parts that cancel divergent parts occurring in loop graphs. The finite parts of Z_p, C will be determined through the renormalization procedures in Sec. V. This expansion preserves the symmetry of the Lagrangian order by order.[14] The parameter λ is used only for power counting and is set equal to 1 in what follows.

The fields σ_0 and σ_8 have nonvanishing vacuum expectation values. It is useful to define new fields S_i:

$$\sigma_i = S_i + (\xi_i + \delta\xi_i) \quad (i=0,8)\,,$$
$$\sigma_i = S_i \quad (i=1,\ldots,7)\,.$$

Note that the parameters ξ_i has its second-order part separated off just as do all other parameters in the model. The $\xi_i+\delta\xi_i$ will be chosen such that $\langle S_i\rangle = 0$ order by order. It is also convenient to define

$$b=\xi_8/\sqrt{2}\,\xi_0, \quad a=\epsilon_8/\sqrt{2}\,\epsilon_0$$

with appropriately defined second-order parts $\delta b, \delta a$. Expressing the Lagrangian in terms of ϕ_i and S_i gives

$$\begin{aligned}\mathcal{L} = C\big[&\tfrac{1}{2}(\partial_\mu\phi_i)^2+\tfrac{1}{2}(\partial_\mu S_i)^2\\ &-\tfrac{1}{2}M^{S2}_{ij}S_iS_j-\tfrac{1}{2}M^{\phi 2}_{ij}\phi_i\phi_j\\ &+\tfrac{1}{6}G^S_{ijk}S_iS_jS_k+\tfrac{1}{2}G^\phi_{ij,k}\phi_i\phi_jS_k\\ &+\tfrac{1}{24}F^S_{ijkl}S_iS_jS_kS_l+\tfrac{1}{24}F^\phi_{ijkl}\phi_i\phi_j\phi_k\phi_l\\ &+\tfrac{1}{4}F^{S\phi}_{ij,kl}\phi_i\phi_jS_kS_l-E_iS_i\big]\,,\end{aligned} \tag{2.6}$$

where

$$\begin{aligned}F^\phi_{ijkl} &= F^S_{ijkl}\\ &\equiv 8f_1Z_{f_1}(\delta_{ij}\delta_{kl}+\delta_{ik}\delta_{jl}+\delta_{il}\delta_{jk})\\ &\quad+4f_2Z_{f_2}(d_{ijn}d_{kln}+d_{ikn}d_{jln}+d_{iln}d_{jkn})\,,\end{aligned} \tag{2.7a}$$

$$\begin{aligned}F^{S\phi}_{ij,kl}&\equiv 8f_1Z_{f_1}\delta_{ij}\delta_{kl}\\ &\quad+4f_2Z_{f_2}(d_{ijn}d_{kln}+f_{ikn}f_{jln}+f_{iln}f_{jkn})\,,\end{aligned} \tag{2.7b}$$

$$G_{ijk}\equiv\frac{1}{\sqrt{2}}\,gZ_g\,\epsilon_{abc}\,\lambda^i_{aa'}\,\lambda^j_{bb'}\,\lambda^k_{cc'}\,\epsilon_{a'b'c'}\,, \tag{2.7c}$$

$$G^S_{ijk}\equiv G_{ijk}+F^S_{ijkl}(\xi_l+\delta\xi_l)\,, \tag{2.7d}$$

$$G^\phi_{ij,k}\equiv -G_{ijk}+F^{S\phi}_{ij,kl}(\xi_l+\delta\xi_l)\,, \tag{2.7e}$$

$$M^{S2}_{ij}\equiv\mu^2Z_\mu\delta_{ij}-G_{ijk}\xi_k-\tfrac{1}{2}F^S_{ij,kl}\xi_k\xi_l-G^S_{ijk}\delta\xi_k\,, \tag{2.7f}$$

$$M^{\phi 2}_{ij}\equiv\mu^2Z_\mu\delta_{ij}+G_{ijk}\xi_k-\tfrac{1}{2}F^{S\phi}_{ij,kl}\xi_k\xi_l+G^\phi_{ij,k}\delta\xi_k\,, \tag{2.7g}$$

$$E_i\equiv\epsilon_iZ_{\epsilon_i}+\mu^2Z_\mu\xi_i-\tfrac{1}{2}G_{ijk}\xi_j\xi_k-\tfrac{1}{6}F^S_{ijkl}\xi_j\xi_k\xi_l+M^{S2}_{ij}\delta\xi_j\,. \tag{2.7h}$$

All sums go over 0 to 8. Note that M, G, F, and E have second-order parts. Since we are only working to second order, it is understood that in Eqs. (2.6) and (2.7) all expressions are to be truncated to that order.

B. Tree approximation

We start by first solving the model in the tree approximation, i.e., truncating Eqs. (2.6) and (2.7) to lowest order. This involves finding a vacuum, determining the masses and coupling constants, and fitting the model to physical masses and decay constants. Feynman rules for higher orders are then expressed in terms of these solutions.

The vacuum state is chosen such that $\langle S_i\rangle=0$, which implies $E_i=0$. Combining Eqs. (2.7h) and (2.7g) gives

$$\begin{aligned}\epsilon_0(1+a)&=-m_\pi^2\,\xi_0(1+b)\,,\\ \epsilon_0(1-a/2)&=-m_K^2\,\xi_0(1-b/2)\,.\end{aligned} \tag{2.8}$$

The decay constants f_K and f_π are simply related to these expressions:

$$\begin{aligned}f_\pi m_\pi^2&=-(\tfrac{2}{3})^{1/2}\epsilon_0(1+a)\,,\\ f_Km_K^2&=-(\tfrac{2}{3})^{1/2}\epsilon_0(1-a/2)\,.\end{aligned} \tag{2.9}$$

The masses are obtained from Eqs. (2.7f) and (2.7g). There is 0–8 mixing which we diagonalize to this order:

$$\begin{aligned}R^\phi_{i\alpha}M^\phi_{ij}R^\phi_{j\beta}&=M^{\phi 2}_\alpha\delta_{\alpha\beta}\,,\\ R^S_{i\alpha}M^{S2}_{ij}R^S_{j\beta}&=M^{S2}_\alpha\delta_{\alpha\beta}\,,\end{aligned} \tag{2.10}$$

where

$$R^\phi_{i\alpha}=\begin{array}{c}\\ 8\\ 0\end{array}\begin{array}{c}\begin{array}{cc}\eta & \eta'\end{array}\\ \begin{pmatrix}\cos\theta_P & \sin\theta_P\\ -\sin\theta_P & \cos\theta_P\end{pmatrix}\end{array}\,,$$

$$R^S_{i\alpha}=\begin{array}{c}\\ 8\\ 0\end{array}\begin{array}{c}\begin{array}{cc}\sigma' & \sigma\end{array}\\ \begin{pmatrix}\cos\theta_S & \sin\theta_S\\ -\sin\theta_S & \cos\theta_S\end{pmatrix}\end{array}\,. \tag{2.11}$$

We conform to the convention that in the diagonal basis Greek indices will be used. For example, if O_i is an object with an SU_3 index, then in the diagonal basis we denote it $O_\alpha = R_{i\alpha} O_i$.

The fitting procedure works as follows:

$$\left.\begin{matrix} m_\pi \\ m_K \\ m_\eta \\ m_{\eta'} \end{matrix}\right\} \text{ determines } \left\{\begin{matrix} \mu^2 - 4\xi_0^2(1+2b^2)f_1 \\ \xi_0^2 f_2 \\ \xi_0 g \\ b \end{matrix}\right. \quad (2.12)$$

From this, m_{π_N}, m_κ, θ_P, and f_K/f_π are fixed. Next m_σ (lower isoscalar) fixes μ^2, which in turn determines $m_{\sigma'}$ and θ_S. Finally ξ_0 is determined in terms of f_π through Eqs. (2.8) and (2.9). The symmetry-breaking parameters are given by Eq. (2.8). This completes the fit except for one notable qualification: For $-0.35 \lesssim b \lesssim -0.15$, m_K changes by only a few MeV. Since the K^+-K^0 mass difference is of this order, we can consider b a bonus parameter over a large range (see paper I for more detail).

The Feynman rules are given in Fig. 1 in the diagonalized basis. Note from Eq. (2.7a) that $F^S_{ijkl} = F^\phi_{ijkl}$; however, $F^S_{\alpha\beta\gamma\delta} \neq F^\phi_{\alpha\beta\gamma\delta}$ since the scalars and pseudoscalars are diagonalized by different rotations.

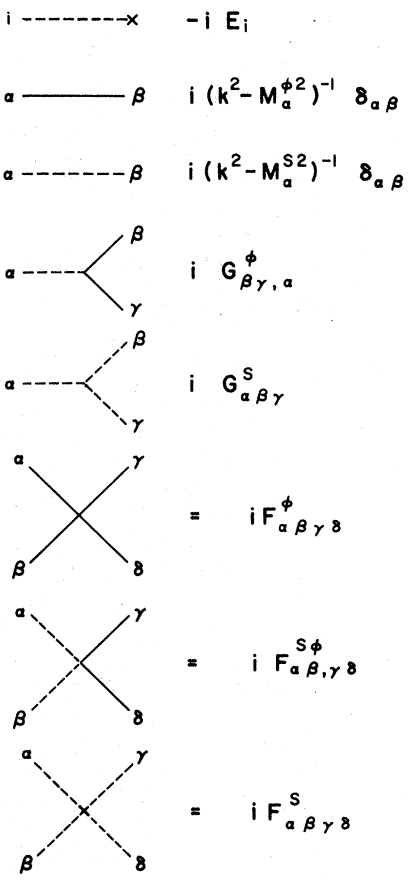

FIG. 1. Feynman rules. Solid lines are pseudoscalars; dashed lines are scalars. The Greek indices indicate that the isoscalars are diagonalized to the tree order. $F^S_{\alpha\beta\gamma\delta} \neq F^\phi_{\alpha\beta\gamma\delta}$ since the scalar and pseudoscalar mixing angles are different.

III. WARD IDENTITIES

There are numerous Ward identities among the n-point functions that follow from chiral symmetry and PCAC. These identities are useful in identifying model-independent relations. Coupled with our specific renormalization procedure we are able to identify quantities that have no second-order correction. Further, some of the relations presented here were used to check our calculations.

We first summarize the needed operator relations. These all follow from standard Lagrangian machinery and can be found in Ref. 2, for example. As a consequence of the assignment of the M^0 fields to the $(3, \bar{3})$ representation, we have the commutation relations

$$\begin{aligned} &[Q_i^V, \phi_j^0] = i f_{ijk} \phi_k^0, \\ &[Q_i^V, \sigma_j^0] = i f_{ijk} \sigma_k^0, \\ &[Q_i^A, \phi_j^0] = i d_{ijk} \sigma_k^0, \\ &[Q_i^A, \sigma_j^0] = -i d_{ijk} \phi_k^0, \end{aligned} \quad (3.1)$$

where Q_i^V and Q_i^A are the vector and axial-vector charges,

$$Q_i^{(V,A)} = \int d^3x (V_i^0(x), A_i^0(x)), \quad (3.2)$$

with the standard commutation relations

$$\begin{aligned} &[Q_i^V, Q_j^V] = i f_{ijk} Q_k^V, \\ &[Q_i^V, Q_j^A] = i f_{ijk} Q_k^A, \\ &[Q_i^A, Q_j^A] = i f_{ijk} Q_k^V. \end{aligned} \quad (3.3)$$

The divergence of the axial-vector current satisfies the operator relation

$$\partial_\mu A_i^\mu = i[Q_i^A, \mathcal{L}_{SB}] = -d_{ijk} \epsilon_j^0 \phi_k^0 \quad (i = 1, 8; j, k = 0, \ldots, 8). \quad (3.4)$$

Finally, we need the renormalized fields defined by

$$\langle 0 | \phi_a^R(0) | a \rangle = \frac{1}{(2\pi)^{3/2}(2P_a^0)^{1/2}} \quad (3.5)$$

[$a = (1, \ldots, 7, \eta, \eta')_P$, where the subscript P refers to the physical states]. The relation between ϕ^R

and ϕ^0 is

$$\phi_a^R = Z_{ia}{}^{-1/2}\phi_i^0 \tag{3.6}$$

(see Table I). We do not renormalize the scalar fields, since the scalars are unstable. Strictly speaking, we cannot renormalize the η' field, for the same reason. However, to the order of approximation in which we work, the η' is stable. $Z_{ia}{}^{-1/2}$ is diagonal except for η-η', 0–8 mixing. It is determined by Eq. (3.5) or in terms of propagators:

$$D_{ij}^0 = Z_{ia}{}^{1/2} D_{ab}^R Z_{jb}{}^{1/2}, \tag{3.7}$$

where

$$D_{ab}^R(s \to m_a^2) \sim \frac{\delta_{ab}}{s - m_a^2}.$$

Table I summarized the renormalizations introduced up to now together with conventions in notation. (The chiral-invariant renormalization is not used in this section.)

We define the decay constants f_{ia} as follows[15]:

$$\partial_\mu A_i^\mu = \sum_{a=0}^{8} f_{ia} m_a^{\phi 2} \phi_a^R \quad (i = 1, \ldots, 8). \tag{3.8}$$

More explicitly,

$$\partial_\mu A_i^\mu = \begin{cases} f_\pi{}^2 m_\pi{}^2 \phi_a^R & (i = a = 1, 2, 3), \\ f_K m_K{}^2 \phi_a^R & (i = a = 4, 5, 6, 7), \\ f_{8\eta} m_\eta{}^2 \phi_\eta^R + f_{8\eta'} m_{\eta'}{}^2 \phi_{\eta'}^R & (i = 8). \end{cases} \tag{3.9}$$

Equations (3.4), (3.6), and (3.8) give

$$f_{ia} m_a^{\phi 2} = -d_{ijk} \epsilon_j^0 Z_{ka}{}^{1/2} \quad (i \neq 0). \tag{3.10}$$

In terms of the renormalized fields, the commutation relations with the axial charges are

$$\begin{aligned} [Q_i^A, \phi_a^R] &= i d_{ijk} Z_{ja}{}^{-1/2} \sigma_k^0, \\ [Q_i^A, \sigma_j^0] &= -i d_{ijk} Z_{ka}{}^{1/2} \phi_a^R. \end{aligned} \tag{3.11}$$

Equations (3.8) and (3.11) are the key inputs to the Ward identities.

The identity linking the two-point and one-point function starts from the relation

$$\begin{aligned} \partial_\mu \langle T(A_i^\mu(x) \phi_a^R(0)) \rangle \\ = \langle T(\partial_\mu A_i^\mu(x) \phi_a^R(0)) \rangle + \delta(x^0) \langle [A_i^0(x), \phi_a^R(0)] \rangle. \end{aligned} \tag{3.12}$$

Take the Fourier transform $\int d^4x\, e^{ip\cdot x}$ and let $p^\mu \to 0$. The left-hand side is zero and the right-hand side becomes

$$0 = i \sum_b f_{ib} m_b^{\phi 2} D_{ba}^R(p^2 = 0) + \langle [Q_i^A, \phi_a^R] \rangle, \tag{3.13}$$

where D^R is the pseudoscalar propagator (see Table I). Using Eq. (3.11) gives

$$f_{ib} m_b{}^2 = -\sum_{jka} d_{ijk} Z_{ja}{}^{-1/2} \langle \sigma_k^0 \rangle D_{ab}^{R-1}(0). \tag{3.14}$$

Since the left-hand side is proportional to symmetry-breaking parameters in the Lagrangian, we recognize Eq. (3.14) as a statement of the Goldstone theorem.

An identity involving the three-point function follows from the same manipulations, starting with

$$\frac{\partial}{\partial x^\mu} \langle T(A_i^\mu(x) \phi_a^R(y) \sigma_k^0(z)) \rangle.$$

The identity is

$$\begin{aligned} \sum_{bc} f_{ib} m_b{}^2 D_{bc}^R(0) \langle c | \sigma_k^0(0) | a \rangle |_{p_c = 0} \\ = -\sum_{jlb} d_{ijl} Z_{jb}{}^{-1/2} D_{ba}^{R-1}(q_a{}^2) \tilde{\Delta}_{lk}^0(q_a{}^2) \\ + \sum_l d_{ikl} Z_{la}{}^{1/2}. \end{aligned} \tag{3.15}$$

(See Table I for the meaning of $\tilde{\Delta}$.) Evaluating this in the tree approximation and taking $q_a{}^2$ equal to appropriate scalar masses, this gives a useful expression for the pseudoscalar-pseudoscalar-scalar coupling constants in terms of decay constants, masses, and mixing angles. These were used in Sec. IV.

A four-point-function identity given below is obtained, starting with $\partial_\mu \partial_\nu \langle (A^\mu A^\nu \phi \phi) \rangle$:

$$\begin{aligned} \sum_{cdc'd'} f_{id} m_d{}^2 f_{jc} m_c{}^2 D_{cc'}^R(0) D_{dd'}^R(0) \langle ac' | T | bd' \rangle |_{\substack{q_{c'} = q_{d'} = 0 \\ q_a = q_b = q}} \\ = -\sum_{cl} f_{jc} m_c{}^2 d_{ilk} Z_{lc}{}^{-1/2} \langle a | \sigma_k^0(0) | b \rangle + \Big[-\sum_{klmna'b'} d_{imk} Z_{ma'}{}^{-1/2} d_{jnl} Z_{nb'}{}^{-1/2} \tilde{\Delta}_{lk}(q^2) D_{a'a}^{R-1}(q^2) D_{b'b}^{R-1}(q^2) \\ + \sum_{klmna'} d_{imk} Z_{ma'}{}^{-1/2} D_{a'a}^{R-1}(q^2) d_{jkn} Z_{nb}{}^{1/2} + (a \leftrightarrow b) \Big]. \end{aligned} \tag{3.16}$$

If we take q_a and q_b on the mass shell, the term in square brackets is zero, giving a relation between the partly off-shell scattering amplitude and the on-shell matrix elements of the σ field. Our interest in this expression lies in isolating quantities that have no second-order corrections. We wish to choose external labels such that the $\langle a|\sigma|b\rangle$ terms vanish. This is only possible if we restrict the external labels to π's and K's, in which case the expression greatly simplifies.

$\pi_a\pi_c \to \pi_b\pi_d$; $p_d = p_d = 0$; $p_a = p_b = q$.

$$T_{ac,bd} f_\pi{}^2 [m_\pi{}^2 D_\pi^R(0)]^2 = [D_\pi^{R-1}(q^2) + O((q^2 - m_\pi{}^2)^2)](\delta_{ac}\delta_{bd} + \delta_{ad}\delta_{bc}) + O(\text{const})\,\delta_{ab}\delta_{cd} \tag{3.17}$$

for $q^2 \approx m_\pi{}^2$. Decompose the $\pi\pi$ amplitude in the standard way,

$$T_{ac,bd} = T^s \delta_{ac}\delta_{bd} + T^t \delta_{ab}\delta_{cd} + T^u \delta_{ad}\delta_{bc}. \tag{3.18}$$

The kinematical constraints for the Ward's identity are $s = u = q^2$, $t = 0$. Hence $T^s = T^u$. The identity then gives

$$[m_\pi{}^2 D_\pi^R(0)]^2 T^s = \frac{1}{f_\pi{}^2}[q^2 - m_\pi{}^2 + O((q^2 - m_\pi{}^2)^2)]. \tag{3.19}$$

For tree graphs, $T^s = (q^2 - m_\pi{}^2)/f_\pi{}^2 + O((q^2 - m^2)^2)$. *Since we renormalize at f_π and $m_\pi{}^2$, we conclude that the higher-order corrections to $[m_\pi{}^2 D_\pi^R(0)]^2 T^s$ have a double zero at $q^2 = m_\pi{}^2$.* Since the corrections to $D_\pi^R(0)$ are extremely small, the same statement holds for T^s for all practical purposes. That is, the higher-order corrections to $T_s \sim O((q^2 - m^2)^2) + \zeta$ $(\zeta \ll 1)$. *Having found a point where the tree approximation is exact, we claim that perturbation theory should be better the closer you are to this point, i.e., low energies.*

$K_a K_c \to K_b K_d$; $p_c = p_d = 0$; $p_a = p_b = q$.

$$f_K{}^2 [m_K{}^2 D_K^R(0)]^2 T_{acbd} = O(\text{const}) \sum_{m=1}^{3} d_{abm} d_{cdm} + O(\text{const})\,\delta_{ab}\delta_{cd} + [(q^2 - m_K{}^2) + O((q^2 - m_K{}^2)^2)](\delta_{ac}\delta_{bd} + \delta_{ad}\delta_{bc}) \tag{3.20}$$

for $q^2 \sim m_K{}^2$. We take the following decomposition of the KK-KK amplitude:

$$T_{ac,bd} = A^s \delta_{ac}\delta_{bd} + A^t \delta_{ab}\delta_{cd} + A^u \delta_{ad}\delta_{bc} + B^s f_{ac8} f_{bd8} + B^t f_{ab8} f_{dc8} + B^u f_{ad8} f_{cb8}. \tag{3.21}$$

A^s (B^s) is symmetric (antisymmetric) under t-u crossing. Analogous crossing properties hold for the remaining amplitudes. At the point $t = 0$,

$s = u = q^2$

$$B^t = 0, \quad B^s = -B^u, \quad A^s = A^u.$$

Using Eq. (3.21), the Ward identity (3.20) gives

$$f_K{}^2 [m_K{}^2 D_K^R(0)]^2 (A^s - \tfrac{3}{4} B^s) = (q^2 - m_K{}^2) + O((q^2 - m_K{}^2)^2) \tag{3.22}$$

for $q^2 \sim m_K{}^2$. The tree graphs give

$$f_K{}^2 (A^s - \tfrac{3}{4} B^s) = (q^2 - m_K{}^2) + O((q^2 - m_K{}^2)^2).$$

As for the $\pi\pi$ case, the second- and higher-order corrections to the left-hand side of Eq. (3.22) have a double zero in q^2-$m_K{}^2$. However, for this case the corrections to $D_K^R(0)$ are larger, and we do not renormalize at f_K.

SU_3 *limit, pseudoscalar octet:* $ac \to bd$, $p_c = p_d = 0$, $p_a = p_b = q$.

$$f_{P_8}{}^2 [m_{P_8}{}^2 D_{P_8}^R(0)]^2 \langle ac|T|bd\rangle = O(\text{const})\,\delta_{ab}\delta_{cd} + O(\text{const}) \sum_{m=1}^{8} d_{abm} d_{cdm} + (q^2 - m_{P_8}{}^2) \sum_{m=0}^{8} (d_{acm} d_{bdm} + d_{adm} d_{bcm}) \tag{3.23}$$

for $q^2 \to m_{P_8}{}^2$. We can decompose $T_{ac,bd}$ as follows:

$$T_{ac,bd} = \tilde{A}^s \delta_{ac}\delta_{bd} + \tilde{A}^t \delta_{ab}\delta_{cd} + \tilde{A}^u \delta_{ad}\delta_{bc} + \sum_{m=1}^{8} (\tilde{B}^s d_{acm} d_{bdm} + \tilde{B}^t d_{abm} d_{cdm} + \tilde{B}^u d_{adm} d_{bcm}). \tag{3.24}$$

These six tensors are not independent but satisfy the relation

$$\delta_{ac}\delta_{bd} + \delta_{ab}\delta_{cd} + \delta_{ad}\delta_{bc} = -3 \sum_{m=1}^{8} (d_{acm} d_{bdm} + d_{abm} d_{cdm} + d_{adm} d_{bcm}). \tag{3.25}$$

Hence, $T_{ac,bd}$ is invariant under the replacements

$$\tilde{A} \to \tilde{A} + \Lambda, \quad \tilde{B} \to \tilde{B} - 3\Lambda. \tag{3.26}$$

These can be verified most easily by expanding Eq. (3.25) in a complete set of projection operators which are given in Appendix C. There are, of course, only five independent tensors in the reduction of $P_8 \times P_8$.

Going to the point $s = u = q^2$, $t = 0$, then $\tilde{A}^s = \tilde{A}^u$, $\tilde{B}^s = \tilde{B}^u$, and Eq. (3.23) gives

$$f_{P_8}{}^2 [m_{P_8}{}^2 D_{P_8}^R(0)^{-1}]^2 (\tilde{A}^s + \tilde{B}^s/3) = (q^2 - m_{P_8}{}^2) + O((q^2 - m_{P_8}{}^2)^2). \tag{3.27}$$

One further relation on the scattering amplitude which is of interest results when one four-momentum q_a goes to zero:

$$\sum_a f_{ia} m_a^2 D^R_{aa'}(0)\langle a'c|T|bd\rangle|_{P_a=0}$$
$$=\sum_{b'k} d_{ib'k} D^{R-1}_{b'b}(q_b^2)\langle c|\sigma_k(0)|d\rangle$$
$$+\sum_{c'k} d_{ic'k} D^{R-1}_{c'c}(q_c^2)\langle c|\sigma_k(0)|bd\rangle$$
$$+\sum_{d'k} d_{id'k} D^{R-1}_{d'd}(q_d^2)\langle c|\sigma_k(0)|b\rangle. \quad (3.28)$$

For b, c, and d on the mass shell, this gives the Adler zero.[10] For $s=(q_a+q_c)^2$, $t=(q_a-q_b)^2$, this is the point: $s=q_c^2$, $t=q_b^2$, $u=q_d^2$.

IV. SCATTERING GRAPHS—TREE ORDER

It is worthwhile looking at analytic expressions for the tree graphs. They take a simple form when expressed in terms of masses and decay constants. They exhibit the low-energy theorems described in the previous section. Further, they can be used to indicate the signs and relative strengths of forces in various channels.

A. SU_3 limit

Let us consider P_8-P_8 (pseudoscalar octet) scattering labeled $i+j\to k+l$, $s=(p_i+p_j)^2$, $t=(p_i-p_k)^2$. The sum of tree graphs can be written

$$T_{ijkl}=\tilde{A}^s\delta_{ij}\delta_{kl}+\tilde{A}^t\delta_{ik}\delta_{jl}+\tilde{A}^u\delta_{il}\delta_{jk}$$
$$+\sum_{m=1}^{8}(\tilde{B}^s d_{ijm}d_{klm}+\tilde{B}^t d_{ikm}d_{jlm}+\tilde{B}^u d_{ilm}d_{jkm}), \quad (4.1)$$

where

$$\tilde{A}^x=(m_{P_8}^2-m_{S_0}^2)(x-m_{P_8}^2)/\xi_0^2(x-m_{S_0}^2), \quad (4.2)$$
$$\tilde{B}^x=\tfrac{3}{2}(m_{P_8}^2-m_{S_8}^2)(x-m_{P_8}^2)/\xi_0^2(x-m_{S_8}^2).$$

These six tensors are not independent—as was discussed in Sec. III. Hence, there was a choice involved in writing Eq. (4.1). Changes in $\tilde{A}$ and $\tilde{B}$ given by Eq. (3.26) will, of course not affect T.

If we let $P_i\to 0$, which corresponds to $s=t=u=m_{P_8}^2$, T clearly vanishes as Eq. (3.28) dictates, giving the Adler zero. If we let $p_i=p_k=0$ and $p_j^2=p_l^2=q^2$, corresponding to $s=u=q^2$, $t=0$, we find

$$\tilde{A}^s+\tfrac{1}{3}\tilde{B}^s=(q^2-m_{P_8}^2)/\tfrac{2}{3}\xi_0^2+O((q^2-m_{P_8}^2)^2) \quad (4.3)$$

for $q^2\to m_{P_8}^2$. Since $f_{P_8}=(\frac{2}{3})^{1/2}\xi_0$, this agrees with the Ward identity (3.27).

We can isolate the four-point coupling parts of $\tilde{A}^x$ and $\tilde{B}^x$:

$$\tilde{A}^x:\ (m_{P_8}^2-m_{S_0}^2)/\xi_0^2,$$
$$\tilde{B}^x:\ \tfrac{3}{2}(m_{P_8}^2-m_{S_8}^2)/\xi_0^2. \quad (4.4)$$

Note that as $m_{S_0}, m_{S_8}\to\infty$ for fixed ξ_0, m_{P_8}, s, t, and u, these expressions diverge, whereas Eqs. (4.2) approach finite limits. This exhibits the cancellations of order $M_{S_{0,8}}^2/s$ as described in the Introduction.

Looking now at the SU_3 diagonalization of T in the s channel obtained with the use of the projection operators in Appendix C we find

$$T^1=8\tilde{A}^s+(\tilde{A}^t+\tilde{A}^u)+\tfrac{5}{3}(\tilde{B}^t+\tilde{B}^u),$$
$$T^{8s}=(\tilde{A}^t+\tilde{A}^u)+\tfrac{5}{3}\tilde{B}^s-\tfrac{1}{2}(\tilde{B}^t+\tilde{B}^u),$$
$$T^{27}=(\tilde{A}^t+\tilde{A}^u)+\tfrac{1}{3}(\tilde{B}^t+\tilde{B}^u), \quad (4.5)$$
$$T^{8a}=(\tilde{A}^t-\tilde{A}^u)+\tfrac{5}{6}(\tilde{B}^t-\tilde{B}^u),$$
$$T^{10}=(\tilde{A}^t-\tilde{A}^u)-\tfrac{2}{3}(\tilde{B}^t-\tilde{B}^u).$$

We can make an estimate of the forces in various channels, thinking of these terms as "potentials." For our case of interest $m_{S_0}, m_{S_8}>m_{P_8}$. Of the three S-wave amplitudes, T^1 and T^{8s} are dominated by the scalar-meson poles. T^{27} is negative, indicating repulsion and a negative phase shift (normalized to zero at threshold). For P waves $(\tilde{A}^t-\tilde{A}^u)$ and $(\tilde{B}^t-\tilde{B}^u)$ give a positive $l=1$ projection; hence the octet is attractive and the $\underline{10}$ has less attraction or possibly is repulsive. For the D waves $\tilde{A}^s$ and $\tilde{B}^s$ do not contribute; $(\tilde{A}^t+\tilde{A}^u)$ and $(\tilde{B}^t+\tilde{B}^u)$ correspond to attraction. Hence the singlet has the most attraction, followed by the $\underline{27}$, and finally the octet is the weakest, and possibly is repulsive. This picture appears to be physically realistic with the exception of the strength of the D wave $\underline{8}_s$ and $\underline{27}$. We must tentatively be suspicious of the D wave and will return to this question in Secs. VI and VII.

B. Broken SU_3

A similar analysis can be carried out for broken SU_3. We give the tree graphs for amplitudes involving π's and K's in external lines. The derivation of these expressions is complicated by the 0–8 mixing. Aids to expressing these amplitudes in terms of masses can be found in Ref. 4 or by using the Ward identity (3.15). Our expressions involve the scalar-mass mixing angle θ_S. Although this angle could be expressed in terms of masses we found no enlightenment results from doing so. The scalar mixing angle θ_S enters in these expressions in the following forms:

$$\gamma_{\sigma'}^{\pi\pi} = (\tfrac{1}{3})^{1/2}\cos\theta_S - (\tfrac{2}{3})^{1/2}\sin\theta_S = -\sin(\theta_S - \theta_c),$$
$$\gamma_{\sigma}^{\pi\pi} = (\tfrac{1}{3})^{1/2}\sin\theta_S + (\tfrac{2}{3})^{1/2}\cos\theta_S = \cos(\theta_S - \theta_c),$$
$$\gamma_{\sigma'}^{K\bar{K}} = (\tfrac{1}{3})^{1/2}\cos\theta_S + 2(\tfrac{2}{3})^{1/2}\sin\theta_S, \tag{4.6}$$
$$\gamma_{\sigma}^{K\bar{K}} = (\tfrac{1}{3})^{1/2}\sin\theta_S - 2(\tfrac{2}{3})^{1/2}\cos\theta_S.$$

The angle θ_c is conventionally called the canonical mixing angle in which the σ' "contains pure strange quarks," $\tan\theta_c = 1/\sqrt{2}$, $\theta_c = 35.3°$. Our θ_S is close to θ_c.

$\pi_i\pi_j \to \pi_k\pi_l$.

$$T_{ijkl} = T^s\delta_{ij}\delta_{kl} + T^t\delta_{ik}\delta_{jl} + T^u\delta_{il}\delta_{jk}, \tag{4.7}$$

$$T^x = \frac{x - m_\pi^2}{f_\pi^2}\left[(\gamma_\sigma^{\pi\pi})^2\frac{m_\pi^2 - m_\sigma^2}{x - m_\sigma^2} + (\gamma_{\sigma'}^{\pi\pi})^2\frac{m_\pi^2 - m_{\sigma'}^2}{x - m_{\sigma'}^2}\right]. \tag{4.8}$$

For $s = u = q^2 \approx m_\pi^2$, $t = 0$,

$$T^s = \frac{q^2 - m_\pi^2}{f_\pi^2} + O((q^2 - m_\pi^2)^2).$$

$\pi_i\pi_j \to K_kK_l$.

$$T_{ijkl} = -\frac{\delta_{ij}\delta_{kl}}{2f_Kf_\pi}\left\{(s - m_\pi^2)\left(\gamma_\sigma^{\pi\pi}\gamma_\sigma^{K\bar{K}}\frac{m_K^2 - m_\sigma^2}{s - m_\sigma^2} + \gamma_{\sigma'}^{\pi\pi}\gamma_{\sigma'}^{K\bar{K}}\frac{m_K^2 - m_{\sigma'}^2}{s - m_{\sigma'}^2}\right)\right.$$
$$\left. - (m_\kappa^2 - m_\pi^2)(m_\kappa^2 - m_K^2)\left[\frac{1}{m_K^2 - m_\kappa^2} - \frac{1}{2}\left(\frac{1}{t - m_\kappa^2} + \frac{1}{u - m_\kappa^2}\right)\right]\right\}$$
$$- \frac{\epsilon_{ijm}f_{klm}}{2f_Kf_\pi}(m_\kappa^2 - m_\pi^2)(m_\kappa^2 - m_K^2)\left(\frac{1}{t - m_\kappa^2} - \frac{1}{u - m_\kappa^2}\right). \tag{4.9}$$

This amplitude vanishes at two different Adler points: i.e., at $s = m_\pi^2$, $t = u = m_K^2$, and $s = m_K^2$, $t = u = m_\pi^2$.

$K_iK_jK_kK_l$.

$$T_{ijkl} = C^s\delta_{ij}\delta_{kl} + C^t\delta_{ik}\delta_{jl} + C^u\delta_{il}\delta_{jk} + \sum_{m=1}^{3}(D^s d_{ijm}d_{klm} + D^t d_{ikm}d_{jlm} + D^u d_{ilm}d_{jkm}); \tag{4.10}$$

$$C^x = \frac{x - m_K^2}{4f_K^2}\left[(\gamma_\sigma^{K\bar{K}})^2\frac{m_K^2 - m_\sigma^2}{x - m_\sigma^2} + (\gamma_{\sigma'}^{K\bar{K}})^2\frac{m_K^2 - m_{\sigma'}^2}{x - m_{\sigma'}^2}\right], \tag{4.11}$$

$$D^x = \frac{x - m_K^2}{f_K^2}\frac{m_K^2 - m_{\pi_N}^2}{x - m_{\pi_N}^2}.$$

Although there are six independent tensors T_{abcd}, the six shown are not independent, i.e., the tree graphs do not contribute in the most general way. The relation between these tensors is

$$(\delta_{ij}\delta_{kl} + \delta_{ik}\delta_{jl} + \delta_{il}\delta_{jk}) - 4\sum_{m=1}^{3}(d_{ijm}d_{klm} + d_{ikm}d_{jlm} + d_{ilm}d_{jkm}) = 0$$
$$(i,j,k,l, = 4, 5, 6, 7). \tag{4.12}$$

The C's and D's are a natural set of amplitudes for tree graphs having isospin-0 and -1 exchange. To compare with the Ward identity, let us convert to the A and B amplitudes of Eq. (3.21):

$$A^s = C^s + \tfrac{1}{4}(D^t + D^u - D^s),$$
$$B^s = \tfrac{1}{3}(D^t - D^u). \tag{4.13}$$

The remaining amplitudes are obtained by cyclic permutation of s, t, u. The Ward identity (3.22) gives a condition on

$$A^s - \tfrac{3}{4}B^s = C^s + \tfrac{1}{4}(2D^u - D^s). \tag{4.14}$$

At the point $s = u = q^2$, $t = 0$, then $D^s = D^u$. We find then, for $q^2 \sim m_K^2$,

$$A^s - \tfrac{3}{4}B^s = C^s + \tfrac{1}{4}D^s = (q^2 - m_K^2) + O((q^2 - m_K^2)^2), \tag{4.15}$$

thereby checking Eq. (3.22).

V. SECOND ORDER

In this section we describe the second-order calculation. This includes loop graphs and the determination of second-order counterterms δC, δZ_p, and $\delta\xi_i$. These are fixed by choosing a set of quantities at which to renormalize. We follow closely the procedure in paper I emphasizing departures. The procedure is outlined in Sec. V A; we leave the details to Sec. V B.

A. Outline of renormalization

The divergences in the loop contributions can be canceled by assigning infinite parts to Z_{f_i}, Z_g, and Z_μ. These infinite parts denoted DZ_p

are derived in Ref. 5 and are given below:

$$
\begin{aligned}
&Z_p = 1 + \delta Z_p ,\\
&\delta Z_p = DZ_p + \Delta Z_p ,\\
&DZ_{f_1} = 8(13 f_1 + 3 f_2^2/f_1 + 12 f_2) B_0(\nu^2) ,\\
&DZ_{f_2} = 48(f_1 + f_2) B_0(\nu^2) ,\\
&DZ_g = 24(f_1 - f_2) B_0(\nu^2) ,\\
&DZ_\mu = 16(g^2/\mu^2) B_0(\nu^2) - [(8 f_1 + 48 f_2)/\mu^2]\\
&\qquad \times [A(\nu^2) + (\mu^2 - \nu^2) B_0(\nu^2)] ,
\end{aligned}
\tag{5.1}
$$

where

$$
\begin{aligned}
A(\nu^2) &= i \int \frac{d^4k}{(2\pi)^4} \frac{1}{k^2 - \nu^2 + i\epsilon} ,\\
B_0(\nu^2) &= i \int \frac{d^4k}{(2\pi)^4} \frac{1}{(k^2 - \nu^2 + i\epsilon)^2}\\
&= \frac{d}{d\nu^2} A(\nu^2) .
\end{aligned}
\tag{5.2}
$$

The parameter ν^2 is chosen arbitrarily; changes in ν^2 merely change the definition of ΔZ_p. The following recipe rids the model of infinities to second order: Subtract the proper combination of $A(\nu^2)$ and $B_0(\nu^2)$ from each divergent integral to make it finite and at the same time write $\delta Z_p = DZ_p + \Delta Z_p$, and discard the DZ_p. All physical quantities are independent of ν^2, which supplies a check on the algebra.

The renormalization procedure must fix C, Z_{f_1} Z_{f_2}, Z_g, Z_μ, Z_{ϵ_0}, Z_{ϵ_8}, $\delta\xi_0$, $\delta\xi_8$, which we choose as follows:

(i) One-point function—two relations. The vanishing of $\langle S_0 \rangle$ and $\langle S_8 \rangle$ must be achieved to this order.

(ii) Mass renormalizations—four relations. We choose to renormalize at the π, K, η, and η' masses.

(iii) Decay constant—one relation. We can renormalize at f_π or f_K but not at both. We choose f_π to have no second-order corrections.

(iv) Symmetry-breaking parameter—one relation. The choice of the value of C does not affect any physical parameters since it is an overall factor in the Lagrangian. We choose it such that $(\frac{2}{3})^{1/2}\epsilon_0 + (\frac{1}{3})^{1/2}\epsilon_8$ has no second-order corrections. This parameter measures the breaking of $SU_2 \times SU_2$ symmetry. This choice corresponds to choosing $C = Z_\pi$ where Z_π is the conventional wave-function renormalization constant of the pion field $\phi^0 = Z_\pi^{1/2} \phi^R$ (see Table I).

(v) Four-point function—one relation. The above eight relations determine C, Z_{f_2}, Z_g, Z_{ϵ_0}, Z_{ϵ_8}, $\delta\xi_0$, $\delta\xi_8$ and the second-order part of

$$
Q + \delta Q = \{\mu^2 Z_\mu - 4(\xi_0 + \delta\xi_0)^2 [1 + 2(b + \delta b)^2] f_1 Z_{f_1}\}/C ,
\tag{5.3}
$$

but not Z_μ and Z_{f_1} separately. This follows from the fact that the pseudoscalar masses in the tree order depend on the combination $Q = [\mu^2 - 4\xi_0^2 \times (1 + 2b^2) f_1]$ but not μ^2 and f_1 separately as was pointed out in Eq. (2.12). Some of the quantities we calculate depend on Z_μ and Z_{f_1} only in the combination (5.3). These will be pointed out in Sec. VI. All scattering amplitudes depend on Z_μ and Z_{f_1} separately.

In paper I we renormalized the σ mass by requiring the real part of the inverse propagator to vanish at the tree mass in order to determine Z_μ and Z_{f_1}. Since the scattering amplitude gives a description of the σ that is superior to the self-energy graphs at this order of approximation, this procedure was changed. We search for a "natural" quantity at which to renormalize, with some difficulty. The σ is so wide that it is difficult to renormalize at its mass in a meaningful way. One possibility is to renormalize at the point $s = t = u = \frac{4}{3} m_\pi^2$ in the $\pi^0\pi^0 \to \pi^0\pi^0$ amplitude. However, since there are trilinear couplings in the model, this point is not interpretable as a 4π coupling constant. We choose to determine Z_{f_1} (and hence Z_μ) by renormalizing at the $\pi\pi$ $I = 0$, $l = 0$ scattering amplitude at an on-mass-shell low-energy point. The loop graphs have a threshold cusp that is absent in the tree graphs. However, this model has phenomenal cancellations at threshold and the cusp effect is greatly suppressed. There are numerous quantities calculated in this paper that do not depend on Z_{f_1} such as decay constants, symmetry-breaking parameters, and wave-function renormalization constants which we will point out later on.

B. Details of renormalization

Now to the details: We start with the conditions that the scalar fields satisfy $\langle S_0 \rangle = \langle S_8 \rangle = 0$. These equations are

$$
CE_i - \tfrac{1}{2} \sum_\alpha [G^S_{\alpha\alpha i} \bar{A}(M_\alpha^2) + G^\phi_{\alpha\alpha,i} \bar{A}(M_\alpha^{\phi 2})] = 0
\qquad (i = 0, 8) .
\tag{5.4}
$$

The loop graphs are shown in Fig. 2(a). E_i, G, and M_α^2 are given in Eq. (2.7). [Note the meaning of Latin and Greek indices in the discussion following Eq. (2.11) and in Table I.] The lowest-order part of E_i is zero from the tree solutions, giving a relation between the second-order finite parts of E_i and the loop contribution. All the parameters in the loop part are truncated to lowest

order. The subtraction recipe is given above in this section. Explicitly,

$$\bar{A}(x) = A(x) - A(\nu^2) - (x-\nu^2)B_0(\nu^2) = (x-\nu^2)\bar{B}(0;x,\nu^2)\,. \tag{5.5}$$

Next consider the pseudoscalar propagators [the loop contributions are shown in Fig. 2(b)]:

$$D^{-1}{}_{\alpha\beta}(s) = C(s\delta_{\alpha\beta} - M^{\phi 2}_{\alpha\beta}) + \tfrac{1}{2}\sum_{\gamma}\left[F^{\phi}_{\alpha\beta\gamma\gamma}\bar{A}(M^{\phi 2}_{\gamma}) + F^{S\phi}_{\alpha\beta,\gamma\gamma}\bar{A}(M^{S2}_{\gamma})\right] - \sum_{\gamma\delta} G^{\phi}_{\alpha\gamma,\delta}G^{\phi}_{\beta\gamma,\delta}\bar{B}(s;M^{\phi 2}_{\gamma},M^{S2}_{\delta})\,, \tag{5.6}$$

where

$$\bar{B}(p^2;x,y) = i\int \frac{d^4k}{(2\pi)^4}\frac{1}{[(k-p)^2 - x + i\epsilon][k^2 - y + i\epsilon]} - B_0(\nu^2)\,. \tag{5.7}$$

Note that $M^{\phi 2}_{\alpha\beta}$ contain second-order parts; the lowest-order part is diagonal. The mass renormalization equations are

$$D^{-1}{}_{\alpha\alpha}(m_\alpha{}^2) = 0 \quad (\alpha = \pi, K, \eta, \eta')\,. \tag{5.8}$$

The lower-case $m_\alpha{}^2$ refer to the physical masses and are in fact equal to the lowest-order part of $M^{\phi 2}_{\alpha}$ as a result of Eq. (5.8). Since the off-diagonal matrix element $D^{-1}{}_{\eta\eta'}$ is of second order, it would contribute to fourth order in the mass renormalization of η and η' and hence is dropped. With these renormalizations we can write

$$D^{-1}{}_{\alpha\beta} = (s - m_\alpha{}^2)\,\delta_{\alpha\beta} - \Sigma_{\alpha\beta}(s)\,, \tag{5.9}$$

where

$$\Sigma_{\alpha\alpha}(m_\alpha{}^2) = 0\,.$$

We will need the wave-function renormalization constants defined through the relations:

$$\phi_\pi = \left(\frac{Z_\pi}{C}\right)^{1/2}\phi^R_\pi\,,$$
$$\phi_K = \left(\frac{Z_K}{C}\right)^{1/2}\phi^R_K\,, \tag{5.10}$$
$$\phi_\alpha = C^{-1/2}Z_{\alpha a}{}^{1/2}\phi^R_a \quad (\alpha, a = \eta, \eta')\,.$$

The R denotes fields that have propagator poles with unit residue. To find the Z's we write

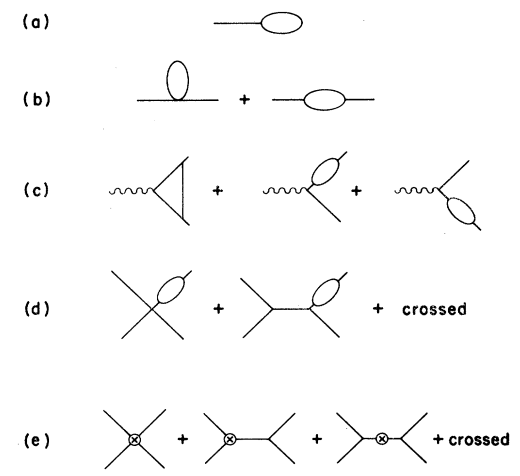

FIG. 2. Loop graphs for (a) one-point function, (b) self-energies, (c) vector form factor, (d) wave-function renormalization, (e) counterterms.

$$D_\pi(s) = \frac{1}{s-m_\pi{}^2} + \frac{1}{s-m_\pi{}^2}\Sigma_\pi(s)\frac{1}{s-m_\pi{}^2} = [1 + \tfrac{1}{2}\Sigma'(m_\pi{}^2)]\,D^R_\pi(s)[1 + \tfrac{1}{2}\Sigma'(m_\pi{}^2)]\,, \tag{5.11}$$

where

$$D^R_\pi(s) = \left[1 + \frac{\Sigma_\pi(s)}{s-m_\pi{}^2} - \Sigma'(m^2)\right]\frac{1}{s-m_\pi{}^2}\,, \tag{5.12}$$

and where Σ' denotes $d\Sigma/ds$. We identify Z_π as

$$Z_\pi = 1 + \Sigma_\pi{}'(m_\pi{}^2) + \delta C = 1 + \sum_{\gamma\delta} G^{\phi}_{1\gamma,\delta}\,G^{\phi}_{1\gamma,\delta}\,\frac{dB}{ds}\,(m_\pi{}^2;M^{\phi 2}_{\gamma},M^{S2}_{\delta})\,. \tag{5.13}$$

Similar expressions hold for the K propagator. The mixed propagator is slightly more involved. With a matrix generalization of Eq. (5.11),

$$D_{\alpha\beta}(s) = C^{-1/2}\,Z_{\alpha a}{}^{1/2}\,D^R_{ab}(s)\,Z_{\beta b}{}^{1/2}\,C^{-1/2}\,, \tag{5.14}$$

$D^R_{ab}(s)$ is defined such that

$$D^R \to \begin{cases} \dfrac{1}{s-m_\eta{}^2}\begin{pmatrix}1&0\\0&0\end{pmatrix} + \text{finite} & (s \to m_\eta{}^2)\,, \\ \dfrac{1}{s-m_{\eta'}{}^2}\begin{pmatrix}0&0\\0&1\end{pmatrix} + \text{finite} & (s \to m_{\eta'}{}^2)\,. \end{cases} \tag{5.15}$$

From these conditions we find

$$Z_{\alpha a}{}^{1/2} = \begin{pmatrix} 1 + \tfrac{1}{2}\Sigma'_{\eta\eta}(m_\eta{}^2) + \dfrac{\delta C}{2} & -\dfrac{\Sigma'_{\eta\eta'}(m_{\eta'}{}^2)}{m_\eta{}^2 - m_{\eta'}{}^2} \\ -\dfrac{\Sigma'_{\eta\eta'}(m_\eta{}^2)}{m_{\eta'}{}^2 - m_\eta{}^2} & 1 + \tfrac{1}{2}\Sigma'_{\eta'\eta'}(m_{\eta'}{}^2) + \dfrac{\delta C}{2} \end{pmatrix}, \tag{5.16}$$

$$D^R_{\eta\eta} = \frac{1}{s-m_\eta^2}\left[1+\Sigma_{\eta\eta}(s)/(s-m_\eta^2)-\Sigma'_{\eta\eta}(m_\eta^2)\right],$$

$$D^R_{\eta'\eta'} = \frac{1}{s-m^2}\left[1+\Sigma_{\eta'\eta'}(s)/(s-m_{\eta'}^2)-\Sigma'_{\eta'\eta'}(m_{\eta'}^2)\right],$$

$$D^R_{\eta\eta'} = \frac{\Sigma_{\eta\eta'}(s)-\Sigma_{\eta\eta'}(m_\eta^2)}{(s-m_\eta^2)(m_\eta^2-m_{\eta'}^2)} + (\eta \rightleftharpoons \eta'). \tag{5.17}$$

Expressions for decay constants are now given to second order. The expression for the divergence of the axial-vector current, Eq. (3.4), when expressed in terms of the variables used in this section, becomes

$$\partial_\mu A_i^\mu = -d_{ijk}(\epsilon_j Z_{\epsilon_j} C^{1/2})(C^{1/2}\phi_k). \tag{5.18}$$

Using Eq. (5.10), this gives for π and K

$$\partial_\mu A_a^\mu = \begin{cases} -[(\frac{2}{3})^{1/2}\epsilon_0 Z_{\epsilon_0}+(\frac{1}{3})^{1/2}\epsilon_8 Z_{\epsilon_8}]\, C^{1/2} Z_\pi^{1/2}\phi_a^R \\ \qquad (a=1,2,3) \\ -[(\frac{2}{3})^{1/2}\epsilon_0 Z_{\epsilon_0}-\frac{1}{2}(\frac{1}{3})^{1/2}\epsilon_8 Z_{\epsilon_8}]\, C^{1/2} Z_K^{1/2}\phi_a^R \\ \qquad (a=4,5,6,7). \end{cases} \tag{5.19}$$

From these and Eq. (3.9) we can identify f_π and f_K:

$$f_\pi m_\pi^2 = -((\tfrac{2}{3})^{1/2}\epsilon_0 Z_{\epsilon_0}+(\tfrac{1}{3})^{1/2}\epsilon_8 Z_{\epsilon_8}) C^{1/2} Z_\pi^{1/2}, \tag{5.20}$$

$$(f_K+\delta f_K) m_K^2 = -((\tfrac{2}{3})^{1/2}\epsilon_0 Z_{\epsilon_0}-\tfrac{1}{2}(\tfrac{1}{3})^{1/2}\epsilon_8 Z_{\epsilon_8}) \times C^{1/2} Z_K^{1/2}. \tag{5.21}$$

Equation (5.20) is one of the defining equations of our renormalization procedure, i.e., $\delta f_\pi = 0$. The lowest-order part of Eq. (5.20) is satisfied at the tree level, Eq. (2.9).

This completes the determination of the second-order parts with the exception of Z_{f_1} (or Z_μ) as discussed above in Sec. V A. We will discuss the determination of Z_{f_1} in Sec. VI, the section on numerical results.

To motivate our choice of C, write the symmetry-breaking part of the Lagrangian as

$$\mathcal{L}_{SB} = -C[(\tfrac{2}{3})^{1/2}\epsilon_0 Z_{\epsilon_0}+(\tfrac{1}{3})^{1/2}\epsilon_8 Z_{\epsilon_8}]\,[(\tfrac{2}{3})^{1/2}\sigma_0+(\tfrac{1}{3})^{1/2}\sigma_8] - C[-(\tfrac{1}{3})^{1/2}\epsilon_0 Z_{\epsilon_0}+(\tfrac{2}{3})^{1/2}\epsilon_8 Z_{\epsilon_8}]\,[-(\tfrac{1}{3})^{1/2}\sigma_0+(\tfrac{2}{3})^{1/2}\sigma_8]. \tag{5.22}$$

The breaking of $SU_2\times SU_2$ is due to the first term; the second term preserves this symmetry. Using Eq. (5.20) and Eq. (2.9) we can write the first term as

$$-\left(\frac{C}{Z_\pi}\right)^{1/2}[(\tfrac{2}{3})^{1/2}\epsilon_0+(\tfrac{1}{3})^{1/2}\epsilon_8]\,[(\tfrac{2}{3})^{1/2}\sigma_0+(\tfrac{1}{3})^{1/2}\sigma_8].$$

Hence by choosing $C=Z_\pi$, the term in brackets which measures $SU_2\times SU_2$ breaking is normalized to the tree value. Using Eq. (2.9) and $C=Z_\pi$, this term can be written

$$f_\pi m_\pi^2[(\tfrac{2}{3})^{1/2}\sigma_0+(\tfrac{1}{3})^{1/2}\sigma_8].$$

C. K_{l3} vector form factor

We wish to calculate in this model the experimentally determined quantity[16]

$$f_K/f_\pi f_+(0) = 1.27\pm 0.03, \tag{5.23}$$

where $f_+(t)$ is the K_{l3} vector form factor. The form factors are defined

$$\sqrt{2}\,\langle\pi^0(p)|\,V^\mu_{4+i5}(0)\,|K^+(q)\rangle = [(p+q)^\mu f_+(t)+(p-q)^\mu f_-(t)], \tag{5.24}$$

where $t=(p-q)^2$. The normalization is such that $f_+(0)=1$ in the SU_3 limit, as follows from the conservation of the vector current. For broken SU_3 we expect it to be very close to 1 as a consequence of the Ademollo-Gatto theorem.[17]

We calculated $f_+(0)$ directly in this model. The graphs entering are shown in Fig. 2(c). Note that there are no counterterm graphs contributing to the vector form factors. This means that it can be calculated directly from the parameters in the tree solution, bypassing the renormalization procedure. In the two-loop order only the one-loop counterterms are needed. Appendixes A and B give expressions for the evaluation of the triangle graph. The form factor $f_+(0)$ was found to be close to one arising from cancellations between the triangle graph and the wave function renormalization graph. The numerical value is given in Sec. VI.

D. Scattering graphs

The scattering graphs are of the following types:

(i) Internal loop graphs. These are given in Fig. 3.

(ii) Graphs with loops on external lines. These types of graphs are given in Fig. 2(d). We are only interested in S-matrix elements and hence these reduce to wave-function renormalization factors on external legs.

(iii) Counterterm graphs. These are given in Fig. 2(e). The x denotes a coupling arising from

the δZ_p or $\delta \xi_i$.

The calculation of all these graphs follow from a straightforward application of the Feynman rules. Considerable labor is involved in calculating the internal loop graphs due to the general mass kinematics. Appendix A gives all these graphs as integrals over discontinuities. By restricting our scope to π, K, and η in external lines and for our σ mass values, there are no anomalous thresholds to worry about. We found a very compact expression for the Box discontinuity function for general masses, Eq. (A6), that we have not seen in the literature and which simplified its evaluation.

E. Partial waves—Padé approximants

The partial-wave projections are defined in terms of the amplitude $A(s,t)$:

$$A_l = \tfrac{1}{2}\int_{-1}^{1} dz A(s,t(z)) P_l(z)\,. \tag{5.25}$$

For coupled channels A_l is a matrix in the channel space. We write

$$A_l = T + S, \tag{5.26}$$

when T and S denote tree and second-order part. Unitarity to second order gives

$$\mathrm{Im}S = T\rho T, \tag{5.27}$$

where ImS refers to discontinuity of S across the normal threshold cut, and ρ is the phase-space matrix,

$$\rho = \begin{pmatrix} \rho_1\theta(s-s_1) & 0 & \cdots \\ 0 & \rho_2\theta(s-s_2) & \\ \cdots & & \cdots \end{pmatrix}, \tag{5.28}$$

$$\rho_i = \frac{1}{32\pi}\{[s-(m_a+m_b)^2][s-(m_a-m_b)^2]\}^{1/2}/s\,, \tag{5.29}$$

where m_a and m_b are the masses of the particles in the ith channel, and where s_i are the ith-channel thresholds.

The [1, 1] matrix Padé approximant is

$$A_l^{[1,1]} = T(T-S)^{-1}T\,. \tag{5.30}$$

This satisfies the unitary equation

$$\mathrm{Im}A_l^{[1,1]-1} = -T^{-1}\mathrm{Im}S\,T^{-1} = -\rho\,, \tag{5.31}$$

or, equivalently,

$$\mathrm{Im}\,A_l^{[1,1]} = A_l^{[1,1]\dagger}\rho A_l^{[1,1]}. \tag{5.32}$$

Spurious left-hand cuts can cause difficulty in this algebraic unitarization of the amplitude. Taking $\pi\pi$ and $K\bar{K}$ channels as examples, the left-hand cut in the KK elements of S starts at $s = 4m_K^2 - 4m_\pi^2$. This arises from the 2π exchange in the $K\bar{K}$ amplitude. Other exchanges, σ, π_N, (2σ), etc., give rise to branch points farther to the left. This branch point gets fed back through the Padé approximant to the $\pi\pi$ element of $A_l^{[1,1]}$, producing a singularity above the $\pi\pi$ threshold that clearly does not belong there. Although this could be a very serious problem, we were able to live with it. The phase shifts behave erratically in small neighborhoods around the branch points. This behavior was sensitive to small changes in parameters and could be averaged out. The comparison of the phase shift from different numbers of channels aided in averaging. For our final set of parameters, the effects of left-hand cuts were negligible. The spurious 2π-exchange left-hand cut was negligible for all parameters we looked at. We believe that this is due to suppression of the 2π-exchange graphs near $t \simeq 4m_\pi^2$ as dictated by the strong cancellations discussed in the introduction.

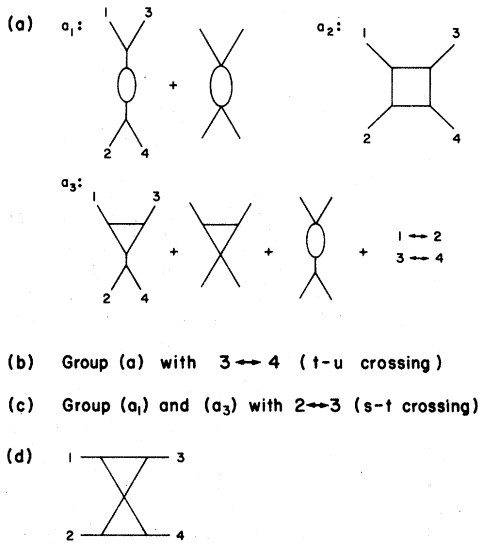

FIG. 3. Second-order scattering graphs characterized by the existence or nonexistence of normal thresholds in the t and u channels. The graphs in (a) have a threshold in t, (b) a threshold in u, (c) threshold in neither t nor u, (d) thresholds in t and u.

F. Expansion parameter

The definition of tree order and second order was given in Eq. (2.5) in terms of an artificial expansion parameter λ. Is there a physical quantity which enters only as a power series param-

eter such as $e^2/\hbar c$ in electrodynamics? The parameter $1/f_\pi{}^2$ serves this purpose. To clarify what we mean, note that coupling constants can be expressed in terms of masses and ξ_0:

$$f_i \sim \frac{\text{mass}^2}{\xi_0{}^2}, \quad g \sim \frac{\text{mass}^2}{\xi_0}.$$

Hence for n-external-line S-matrix elements the ξ_0 dependence (for fixed masses) of tree graphs $T^{(n)}$ is

$$T^{(n)} \sim 1/\xi_0{}^{n-2},$$

and for one-loop graphs $L^{(n)}$,

$$L^{(n)} \sim 1/\xi_0{}^n.$$

Since we renormalize at f_π, we have

$$f_\pi = (\tfrac{2}{3})^{1/2}\xi_0(1+b).$$

Hence these graphs are power series in $1/f_\pi{}^2$. The parameter b is fixed by tree masses. What about counterterm graphs $K^{(n)}$? These contain the quantities Z_p and $\delta\xi_i$ which are determined through the procedure given above. Since we demanded that the second-order part of physical quantities be zero,

$$S^{(n)} = K^{(n)} + L^{(n)} = 0,$$

then clearly $K^{(n)} \sim 1/\xi_0{}^n$.

In summary, since all counterterms are determined by demanding that second-order quantities be zero, i.e., the defining equations are *homogeneous in the order of* λ *(second order)*, our perturbation series is a power series in $1/\xi_0{}^2$ (including the first two terms). Since we renormalize at f_π, and $f_\pi \propto \xi_0$, this is a power series in $1/f_\pi{}^2$.

VI. FIT TO EXPERIMENTAL QUANTITIES—NUMERICAL RESULTS

In this section we present the results of our fit to experimental quantities. There is a vast amount of experimental data to compare with. In order to clarify our method of determining parameters, we first review and expand on all the input that goes into this calculation that has been given earlier in this paper.

A. Input

Table II summarizes the input. The Lagrangian has six parameters. In lowest order these six parameters can be expressed in terms of the six quantities in Table II. In second order, there are six counterterms corresponding to these parameters. Five are determined by renormalizing at the four pseudoscalar masses and at f_π. This fixes Z_{f_2}, Z_g, Z_μ, Z_{ϵ_0}, Z_{ϵ_8} and the combinations of Z_{f_1}, and Z_μ given in Eq. (5.3). We fix the final counterterm, Z_{f_1}, by renormalizing at a low-energy point in the $\pi\pi$ amplitude to be discussed shortly.

The η and η' masses were given their experimental values, the π mass its π^+-π^0 central value. The K mass, however, was taken above its central $K^+ - K^0$ value (by 1%). As mentioned in Sec. II and in more detail in paper I, it was pointed out that although M_K determines $b = \xi_8/\sqrt{2}\,\xi_0$ in principle, a very large range in b leaves M_K almost unchanged (and happily at the physical K mass). The value of $M_K = 502$ MeV gives the tree value $b = -0.16$ and thereby $f_K/f_\pi = (1-b/2)/(1+b) = 1.28$. In paper I we had $M_K = 495$ MeV, $b = -0.25$, $f_K/f_\pi = 1.5$. As we will see, the choice of f_K/f_π in the present paper gives a far better second-order corrected value of $f_K/f_\pi f_+(0)$ and it is for this reason we chose m_K as we did. Since we were aware of the relation between b and m_K in paper I, why did we not choose it then as we do now? The reason lies in the fact that the two-point function description of the lower σ went haywire (σ went below threshold) for $b = -0.16$. The oft-mentioned cancellation at low energies was not present in paper I.

In summary: m_K was not chosen strictly as a fixed input parameter, but was varied to improve $f_K/f_\pi f_+(0)$ at a cost of 1% in the K mass. Why not

TABLE II. Values of all input quantities used for fitting the model at the physical point.

$m_\pi = 138.1$ MeV	
$m_\eta = 548.8$ MeV	
$m_{\eta'} = 958.1$ MeV	
$m_K = 502.1$ MeV	Deviates from experimental K^+-K^0 central mass to improve f_K/f_π (see text).
m_σ(tree) = 775 MeV	Chosen to give best $l = 1, 2$ spectrum and S-wave phase shifts.
$f_\pi = 0.095, 0.120$ GeV	Two values presented. $f_\pi = 0.095$ physical value $f_\pi = 0.120$ chosen to reduce repulsion in exotic $l = 0$ channels.

vary the other masses 1% also? From a pragmatic view it would probably not buy us anything.

The physical value of $f = 0.095$ GeV was used in our fit. However, since f_π determines the overall strength of the forces, we show the effect of increasing f_π, i.e., reducing the strength. The exotic $I = 0$ channels show too much repulsion. We show the cost of decreasing this repulsion on other quantities. Finally this leaves m_σ(tree) which was chosen to get the best overall picture in all the scattering channels.

Table III lists the various parameters calculated to the tree order resulting from the input described above. The parameter a is close to -1, indicating a nearly $SU_2 \times SU_2$ Lagrangian, but since b is small, SU_3 is a good symmetry of states.

This set of tree parameters is such that the model has Goldstone realizations of $SU_3 \times SU_3$ symmetry. At the physical point $\xi_0 = 0.1385$, as shown in Table III. In the $SU_3 \times SU_3$ limit obtained by taking $\epsilon_8, \epsilon_0 \to 0$, $\xi_0 \to 0.113$. The analysis of this limit with regard to the second-order effects will be given in a later paper.

B. Second order—quantities independent of Z_{f_1}

Table IV lists calculated values to second order of decay constants, symmetry-breaking parameters, wave-function renormalization constants, and renormalized propagators at momentum zero. The quantities have the property in common that they do not depend on Z_{f_1}. The quantity $f_K/f_\pi f_+(0)$ has the calculated value 1.34 compared to the experimental value [Eq. (5.23)] 1.27 ± 0.03. Although we could fit this better by decreasing b, it would require more substantial changes in the K mass than the 1% we allowed.

We can understand the size of corrections from a simple *a posteriori* argument. All the quantities in Table IV are proportional to a number e_L which characterizes the strength of loop corrections, which we find to be

$$e_L = \frac{1}{16\pi^2} \frac{M_{P_8}^2}{f_\pi^2} \approx 0.1$$

($M_{P_8} = 400$ MeV as shown in Sec. VI). If the quantity in question goes to zero in the $SU_2 \times SU_2$ limit, the corrections are suppressed by a factor e_2. Similarly, if the corrections go to zero in the SU_3 limit, there is a suppression factor e_3. The numbers e_2 and e_3 can be determined from tree solutions in Table III. Noting that in the $SU_2 \times SU_2$ limit $a = -1$, we estimate

$$e_2 \approx (1 + a) \approx 0.1 ,$$

$$e_3 \approx |b| \approx 0.2 .$$

We can shed some light on the meaning of e_2 by

TABLE III. Quantities calculated to tree order. Those in the first group are fixed by the pseudoscalar masses and f_π; the second group depend also on the choice of m_σ(tree). e_2 and e_3 are explained in the text. For $f_\pi = 0.095$, set $\alpha = 1$.

Quantities independent of m_σ(tree)	$f_\pi = 0.095\alpha$	Order of magnitude
$1 + a = 1 + \epsilon_8/\sqrt{2}\,\epsilon_0$	0.0857	$e_2 \approx 0.1$
$b = \xi_8/\sqrt{2}\,\xi_0$	−0.1600	$e_3 \approx 0.2$
f_K/f_π	1.286	$1 + e_3 \approx 1.2$
$f_{8\eta}/f_\pi$	1.366	$1 + e_3 \approx 1.2$
$f_{8\eta'}/f_\pi$	−0.335	$e_3 \approx 0.2$
θ_P	−2.74°	
m_{π_N} (GeV)	0.966	
m_K (GeV)	1.068	
ϵ_0 (GeV^3)	$-0.025\,88\alpha$	
ξ_0 (GeV)	0.1385α	
f_2	$-6.918\alpha^{-2}$	
g (GeV)	$1.575\alpha^{-1}$	
Quantities dependent on m_σ(tree)	**$f_\pi = 0.095\alpha$**	
$m_{\sigma'}$ (GeV)	1.254	
θ_S	39.7°	
μ^2	−0.1499	
f_1	$-4.668\alpha^{-2}$	

noting

$$1 + a = \frac{f_\pi m_\pi^2}{f_{P_8} m_{P_8}^2} \approx \frac{m_\pi^2}{m_{P_8}^2} \approx 0.1 .$$

The exact equality follows from Eq. (2.9) and the SU_3 limit of Eq. (2.9). Note then that

$$e_2 e_L = \frac{1}{16\pi^2} \frac{m_\pi^2}{f_\pi^2} \approx 0.01 ,$$

which is the order of magnitude expected for corrections to quantities close to the $SU_2 \times SU_2$ limit.

The corrections estimated from these considerations are shown in Table IV, where we see order of magnitude agreement. The last four entries have suppression factors of m_i^2/m_s^2. This follows by noting

$$m_i^2 D_i^R(0) = \frac{m_i^2}{(s - m_i^2)[1 + e_L O((s - m_i^2)/m_s^2)]} \Big|_{s=0} ,$$

since M_s sets the scale of the dispersion integral in the propagator. Our simple argument does not work for the last entry in Table IV. The extrapo-

TABLE IV. Quantities calculated to second order. These are all independent of the value of Z_{f_1}. The quantity $\delta(C\epsilon_0 Z_{\epsilon_0})$ is the correction to the quantity that appears in $\mathcal{L}_{SB}$. We used $C = Z_\pi$. The order of magnitude of corrections is estimated from e_2, e_3, and e_L as described in the text. For $f_\pi = 0.095$, set $\alpha = 1$.

	$f_\pi = 0.095\alpha$	Order of magnitude ($\alpha = 1$)
δa	$-0.00096\alpha^{-2}$	$(1+a)e_2 e_L = 0.001$
δb	$-0.0243\alpha^{-2}$	$b e_L = 0.02$
$\delta(f_K/f_\pi)$	$0.0227\alpha^{-2}$	$e_3 e_L = 0.02$
$\delta(f_{8\eta}/f_\pi)$	$0.0219\alpha^{-2}$	$e_3 e_L = 0.02$
$\delta(f_{8\eta'}/f_\pi)$	$-0.0398\alpha^{-2}$	$e_3 e_L = 0.02$
$\delta(C\epsilon_0 Z_{\epsilon_0})$	$-0.00030\alpha^{-1}$	$\epsilon_0 e_3 e_L = 0.0005$
$\delta\xi_0$	$0.00423\alpha^{-1}$	$\xi_0 e_L = 0.01$
$f_+(0) - 1$	$-0.0221\alpha^{-2}$	$e_3 e_L = 0.02$
$f_K/f_\pi f_+(0)$	$1.286 + 0.051\alpha^{-2}$	
$Z_\pi^{1/2} - 1$	$-0.167\alpha^{-2}$	$e_L = 0.1$
$(Z_K/Z_\pi)^{1/2} - 1$	$0.006\alpha^{-2}$	$e_3 e_L = 0.02$
$[(Z_{\alpha a}{}^{1/2}/Z_\pi{}^{1/2} - \delta_{\alpha a})]$	$\begin{pmatrix} 0.009 & 0.006 \\ -0.029 & 0.067 \end{pmatrix}\alpha^{-2}$	$\begin{pmatrix} e_3 e_L & e_3 e_L \\ e_3 e_L & e_L \end{pmatrix}$
$-m_\pi{}^2 D_\pi^R(0) - 1$	$0.0019\alpha^{-2}$	$e_L m_\pi{}^2/m_S{}^2 = 0.002$
$-m_K{}^2 D_K^R(0) - 1$	$0.0185\alpha^{-2}$	$e_L m_K{}^2/m_S{}^2 = 0.02$
$-m_\eta{}^2 D_\eta^R(0) - 1$	$0.0244\alpha^{-2}$	$e_L m_\eta{}^2/m_S{}^2 = 0.02$
$-m_{\eta'}{}^2 D_{\eta'}^R(0) - 1$	$0.0238\alpha^{-2}$	$e_L m_{\eta'}{}^2/m_S{}^2 = 0.07$

lation of the η' propagator is much closer to a pole extrapolation than one should have expected.

C. S-wave phase shifts

The S-wave phase shifts are given in Figs. 4–7. Those channels that have scalar nonet poles have rising-phase-shift behavior. The exotic channels are all repulsive—characterized by negative phase shifts.

Figure 4 shows the behavior of the $\pi\pi$ S-wave amplitude in the low-energy region. We have chosen Z_{f_1} such that $\mathrm{Re}S_{I=0}^{I=0}(E = 2.2m_\pi) = 0$. Note S_0^0 is very small and has four zeros in this region. $S_0{}^2$ is an order of magnitude smaller. We have also given the sum of all box graphs to show the supression of the cusp effect at threshold when all second-order graphs are added together. This supression is 2 to 3 orders of magnitude. The tree graph result is also plotted along with the Weinberg[18] linear amplitude.

Considerable attention was paid to the $I=0$, $l=0$ phase shifts. Figure 5 illustrates the features seen in this channel. In the region near threshold, the phase shifts for the coupled channel problem approach the single-channel result. We attribute this to the fact that chiral symmetry governs the behavior in this region in a model-independent way. The single-channel phase shift contains an artifact of the approximation. In the notation of Sec. V E the single-channel Padé form is

$$A_l = T^2/(T - S).$$

Since T has two poles (σ, σ'), it has a zero between them. Hence A_l must have the same zero, which accounts for its passage through 180°.

Where is the σ'? We attribute the rising behavior of the $K\bar{K}$ phase shift to the existence of that state much like the σ occurring in $\pi\pi$. This state can be brought near the $K\bar{K}$ threshold, giving the rapid rise to the $\pi\pi$ phase shift much like the experimental situation described by Refs. 19 and 20. However, this is at the cost of destroying everything else.[21] The wiggle in the three-channel phase shifts between 1150 and 1300 MeV is not the σ'. It is a structure that results from repulsion in the $\eta\eta$ channel.

The deviation of two channel and three channel in the $\pi\pi$ case between 550 and 750 MeV we attribute to a spurious left-hand cut arising from the

$\eta\eta$ channel. As we searched over a range of parameters, we found deviations in this region sometimes nonexistent and sometimes wild.

Figure 6 gives our predicted phase shifts for two values of f_π. It was not possible to adjust parameters through reasonable values to get δ_0^0 through 90° at $E = 850$—which would have given a better fit. The inelasticity η in the $\pi\pi$ phase shifts vary from 1 to 0.9 above the $K\bar{K}$ threshold, but since our σ' is not near a threshold (such as the S^*) η is not very interesting.

S-wave scattering lengths, a_0^I, in units of m_π^{-1}, are given in Table V for $\pi\pi$. They are defined

$$a_0^I = m_\pi \lim_{k\to 0} (\delta_0^I/k) \quad (k = \text{c.m. momentum}).$$

The corrections to the $I = 0, 2$ scattering lengths are small, ~1%, as discussed earlier and shown in Fig. 4.

Next consider $\pi\pi$ $I = 2$ in Fig. 6. The phase shift rapidly falls away from the experimental points.[22,23] The repulsion is clearly too strong. In this approximation strong attraction can make bound states or resonances (which are acceptable) but strong repulsion can give rise to phase shifts that fall rapidly through −90° given poles on the physical sheet (which are not acceptable). It is reasonable to believe that in a better approximation the phase shift would not drop as rapidly through −90° but would probably still give too much repulsion to compare favorably with experiment. This repulsion can be decreased by increasing f_π as the dashed curve shows in Fig. 6. However, this has limited effect and further steepens δ_0^0.

The scalar π_N couples to $\pi\eta$ and $K\bar{K}$. The mass and width obtained from the coupled-channel phase shift was $m_{\pi_N} = 840$ MeV, $\Gamma_{\pi_N} \approx 50$ MeV. These are to be compared to the experimental mass of 960 MeV and width of about 30 MeV.

Figure 7 gives the $I = \frac{1}{2}$ and $\frac{3}{2}$ phase shifts. The shaded band above 800 MeV in this figure contains most of the experimental points and was taken from the compilations by Fox and Griss.[24] The shaded region below 800 MeV was taken from a threshold analysis by the same authors. We can estimate the κ pole position from the energy corresponding to the most rapid variation of δ_0^1 which for $f_\pi = 0.095$ gives $M_\kappa \approx 800$, $\Gamma_\kappa \approx 200$. The $I = \frac{3}{2}$ channel, like $I = 2$, suffers from too much repulsion in comparison to the phase-shift analysis of Ref. 25. These are pure $\underline{27}$ channels and this behavior shows up there in the SU_3 limit. The πK scattering lengths are given in Table V.

D. P- and D-wave spectrum

One common feature of models of this type[11] is that the dynamically produced P- and D-wave states have very small widths. Our model is no exception. For this reason we do not give the phase shifts. The existence or nonexistence of states is a measure of the force in these channels which we report here. Table VI gives our results. The P wave seems to be in line with the considerations of the Born terms described in Sec. IV. That is, the $8a$ is resonating and the 10 is not. There can only be one state in the ω, ϕ channel in this approximation which we call ϕ_8. All the states go to

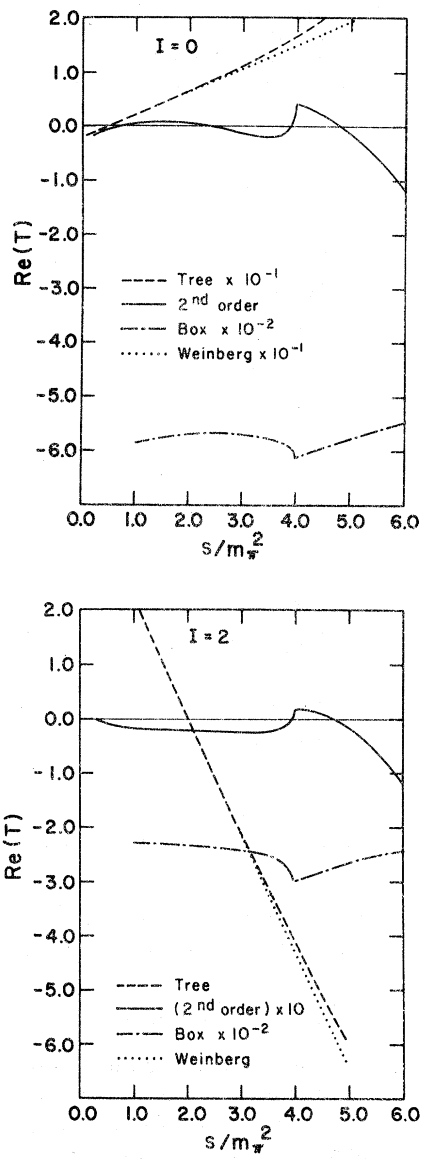

FIG. 4. $\pi\pi$ $I = 0, 2$, $l = 0$ amplitudes in low-energy region. We renormalized the $I = 0$ amplitude at $E = 2.2\ m_\pi$. The linear Weinberg[18] amplitudes are given. Curves labeled "box" are the sum of all box graphs. Note the scale factors for the various functions, $f_\pi = 0.095$ GeV.

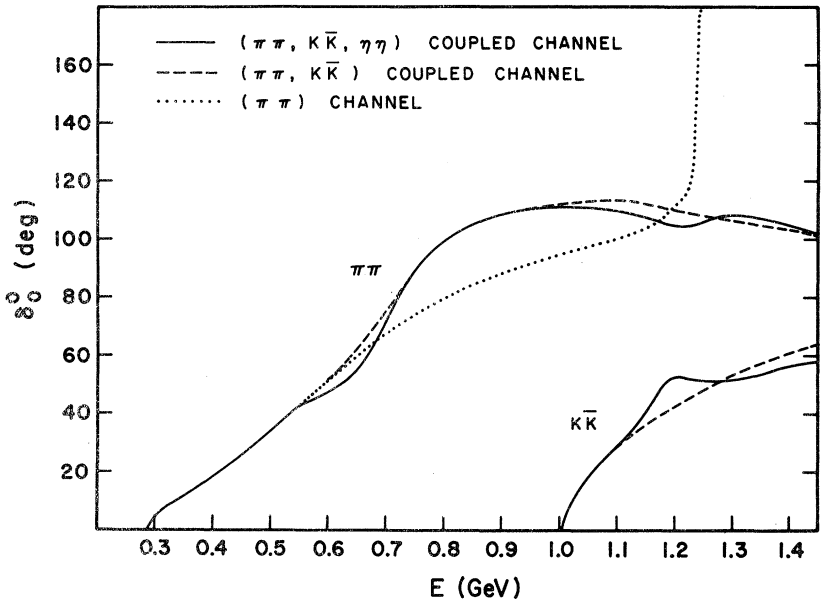

FIG. 5. $I=0$, $l=0$, $\pi\pi$, and $K\bar{K}$ phase shifts for 1, 2, and 3 coupled-channel calculation. The parameters are fixed as given in Table II, $f_\pi = 0.095$ GeV.

higher energy as f_π is increased as expected. The SU_3 mass splitting is small. For those channels that are coupled $\rho \sim (\pi\pi, K\bar{K})$, $K^* \sim (\pi K, \eta K)$, the single-channel result $\rho \sim (\pi\pi)$, $K^* \sim (\pi K)$ gave significantly different masses from those coupled-channel cases. Since SU_3 is clearly a good symmetry for P waves one must at least include all the channels that become degenerate in the exact SU_3 limit in order to get reliable masses.

The results for D waves are given also in Table VI. Here we see that there are exotic states generated for which there are no known resonances. The SU_3 content of these states is traced out in the next section. The upshot is that the lowest of the f, A_2, K^* belong to an octet. This is followed by the 27, and finally the singlet is the highest.

E. Checks

We conclude this section with a list of checks we carried out on this calculation in order to reassure the reader who has gotten this far.

(i) The calculation of paper I was reprogrammed in a systematic fashion and agreed with paper I.

(ii) Generalized Bose symmetry was checked for all full amplitudes (not partial waves).

(iii) Adler zeros were verified for all amplitudes for each external line momentum $P \to 0$.

(iv) The two-point function Ward identity (3.14) was checked.

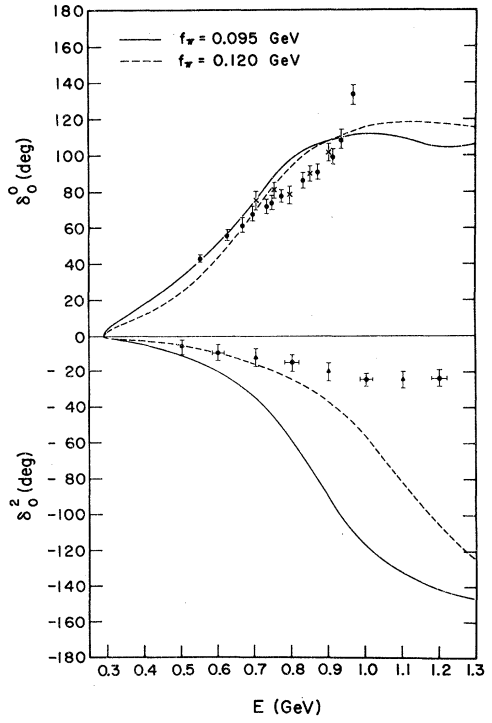

FIG. 6. $\pi\pi$ $I=0$, $I=0,2$ phase shifts. For $I=0$, the dots are taken from Ref. 19, the crosses from Ref. 20. For $I=2$, the dots are taken from Ref. 22, the triangles from Ref. 23.

TABLE V. Scattering lengths a_0^I in units of m_π^{-1}. $\gamma = (1/16\pi)(m_\pi/f_\pi)^2$, $\beta = (1+m_\pi/m_K)^{-1}$. For $f_\pi = 0.095$, $\gamma = 0.042$, $\beta = 0.784$. The entries use $f_\pi = 0.095$ GeV. The column labeled "order of magnitude" is to be compared to the second-order column. e_2 and e_L are defined in the text.

	Weinberg	Tree	Second order	Order of magnitude for second order	Padé approximant
			$\pi\pi$		
$I=0$	$0.147(3.5\gamma)$	$0.168(4.0\gamma)$	$0.001(0.71\gamma^2)$	$a_0^0 e_2 e_L = 0.0017$	0.169
$I=2$	$-0.042(-1\gamma)$	$-0.041(-0.97\gamma)$	$0.0005(0.32\gamma^2)$	$a_0^2 e_2 e_L = 0.0004$	-0.040
			πK		
$I=\frac{1}{2}$	$0.132(4.0\gamma\beta)$	$0.160(4.85\gamma\beta)$	$0.029(20.7\gamma^2\beta)$	$a_0^1 e_L = 0.016$	0.195
$I=\frac{3}{2}$	$0.066(-2.0\gamma\beta)$	$0.054(-1.63\gamma\beta)$	$-0.004(-3.0\gamma^2\beta)$	$a_0^3 e_L = 0.005$	-0.057

(v) The four-point function Ward identity (3.19) and Eq. (3.22) for the $\pi\pi$-$\pi\pi$ and $K\bar{K}$-$K\bar{K}$ amplitudes were checked.

(vi) Coupled channel unitarity for partial waves was checked.

(vii) The program was truncated to give the SU_2 model as described in Ref. 13.

(viii) Invariance of all results on the cutoff mass ν^2 described in Sec. V was checked.

(ix) We checked that the sum of partial waves for $l=0,1,2$ approached the full amplitude.

Checks (ii), (iii), and (v) are good checks on the real part of the amplitude; (iii) and (iv) are good checks on the proper handling of the $\eta\eta'$ mixing; (vi) checks the imaginary part.

VII. SU_3 LIMIT

In this section we give the results of passing to the SU_3 limit. We take the limit in the following way[26]:

$$f_1, f_2, g, \mu^2, \epsilon_0$$

and

$$Z_{f_1}, Z_{f_2}, Z_g, Z_\mu, C$$

fixed at a physical point ($\epsilon_8 \to 0$). This leaves open the determination of $Z_{\epsilon_0}, Z_{\epsilon_8}$, or, equivalently, $\delta\epsilon_0, \delta\epsilon_8$. We felt it was desirable to continue to renormalize at the π and K masses and hence the mass renormalization conditions give two equations for Z_{ϵ_0} and Z_{ϵ_8} as functions of ϵ_8. One could argue that we should hold Z_{ϵ_0} fixed as we pass to the SU_3 limit. This would require that we relax a mass renormalization condition and in the SU_3 limit the P_8 mass would have second-order corrections. The P_8-P_8 threshold would be in the wrong place.

The limit approached this way is a normal limit, meaning $\xi_8, \delta\xi_8, \delta\epsilon_8 \to 0$. Table VII gives the results for many of the quantities of interest. Note that the corrections are all about 10%. Our estimate that they are proportional to e_2 checks out. The near degeneracy of M_{S_0} and M_{S_8} is accidental. Note that f_{P_8} ($=f_K = f_\pi = f_\eta$) and M_{P_0} have second-order corrections since we relaxed these renormalization conditions in this limit. The S-wave phase shifts are shown in Fig. 8. The $\underline{27}$ is strongly repulsive as surmised earlier. It is clear that any future refinements of this model would have to be directed at this excessive repulsion.

Figure 9 is given to untangle the SU_3 content of the dynamically generated P- and D-wave states. Also shown is the pseudoscalar nonet. The ρ, K^*, ϕ_8 states found at the physical point go to the vector octet mass in the SU_3 limit. Hence there is no ambiguity as to the SU_3 content of these

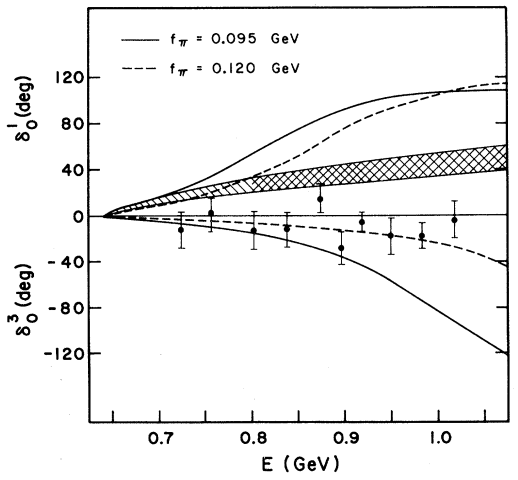

FIG. 7. πK $l=0$, $I=\frac{1}{2}, \frac{3}{2}$ phase shifts. The shaded band represents the experimental points[24] (see text). The dots are $I=\frac{3}{2}$ data points from Ref. 25.

TABLE VI. P- and D-wave spectrum. The column "channels" indicates which channels were coupled together in the matrix Padé amplitude. Masses obtained from a reduced number of coupled channels are given in parentheses. We underline the mass values for the physical value of f_π. States with the same quantum numbers are separated by a slash (/).

	Experiment	$f_\pi = 0.095$	$f_\pi = 0.120$	Coupled channels	
		$J^P = 1^-$			
$I^G = 1^+(\rho)$	770	885	1060	$\pi\pi, K\bar{K}$	only 1 state found
		(645)	(810)	$(\pi\pi)$	
$I^G = 0^-(\phi_8)$	784/1019	910	1033	$K\bar{K}$	only 1 state possible
$I = \frac{1}{2}, Y = 1(K^*)$	892	936	1043	$\pi K, \eta K$	only 1 state found
		(520)	(680)	(πK)	
$I^G = 1^-$			repulsive	$K\bar{K}$	Pure 10
$I = \frac{3}{2}, Y = 1$			repulsive	πK	
$I = 0, Y = 2$			repulsive	KK	
		$J^P = 2^+$			
$I^G = 0^+(f, f')$	1270/1516	1170/1682/1735	1200/1850/1930	$\pi\pi, K\bar{K}, \eta\eta$	
		(1210/1690)	(1270/1920)	$(\pi\pi, K\bar{K})$	
		(1340)	(1485)	$(\pi\pi)$	
$I^G = 1^-(A_2)$	1310	1330/1660	1360/1835	$\pi\eta, K\bar{K}$	
		(1470)	(1580)	$(\pi\eta)$	
$I = \frac{1}{2}, Y = 1(K^{**})$	1421	1110/1710	(1120/1865)	$\pi K, \eta K$	
		(1130)	(1155)	(πK)	
$I^G = 2^+$		1680	1900	$\pi\pi$	Pure 27
$I = \frac{3}{2}, Y = 1$		1605	1800	πK	
$I = 1, Y = 2$		1692	1865	KK	

states—certainly no 10, $\overline{10}$ mixing, which does not resonate. This is in line with the arguments of force strength based on the tree graphs in Sec. IV.

It is interesting that the SU_3 splitting of the vector octet is small. These states are generated dynamically in channels with wildly different thresholds. This is to say that the splitting is probably due to the coupling constants that have symmetry breaking of the order of magnitude of $b = -0.16$ rather than the pseudoscalar masses. The vector octet further exhibits octet dominance of the mass splitting for small values of ϵ_8 as it must. For $\epsilon_8 = 0.3\epsilon_8(\text{physical})$, the Gell-Mann–Okubo mass-squared formula is very well satisfied. For $\epsilon_8 = \epsilon_8(\text{physical})$ the 27 term in the mass breakis clearly important.

For the D wave, the SU_3 assignments of particle states are confused. Note that in the SU_3 limit the states are ordered 8, 27, 1 for increasing mass. This is the reverse order from that estimated from the tree graphs of Sec. IV. The singlet-27 mixing is presumably strong. We cannot associate our SU_3 singlet with the f' since it occurs above the isosinglet member of the 27. Again there is octet dominance of the mass splitting for small ϵ. The ordering of states in mass in the 27 follows the formula $I(I+1) - \frac{1}{4}Y^2$ for small ϵ_8.

VIII. CONCLUSION

It is appropriate in light of this lengthy calculation to review the strengths and weaknesses of this model and the one-loop approximation. The starting point is a Lagrangian based on SU_3 current algebra, operator PCAC, and renormalizability depending on six parameters. Renormalization generates no new parameters. Without the above principles, the number of parameters

TABLE VII. SU_3 limit obtained by taking the physical fit ($f_\pi = 0.095$) and turning off ϵ_8. The quantity C is held fixed at $C = Z_\pi$ (physical point). The order-of-magnitude estimate for all of these corrections is $e_L = 0.1$.

	Tree	Second order
ϵ_0 (GeV^3)	−0.025 88	
$\delta(CZ_{\epsilon_0}\epsilon_0)$ (GeV^3)		0.004 36
ξ_0 (GeV)	0.1457	
$\delta\xi_0$ (GeV)		−0.0155
f_{P_8} (GeV)	0.1190	
δf_{P_8} (GeV)		−0.0169
M_{P_8} (GeV)	0.4214	
M_{P_0} (GeV)	0.9863	
δM_{P_0} (GeV)		0.1476
M_{S_8} (GeV)	1.049	
M_{S_0} (GeV)	1.048	
$Z_{P_8}^{1/2} - 1$		−0.1411
$Z_{P_0}^{1/2} - 1$		−0.0963

in a calculation of this type could be prohibitive. The model is able to fit the pseudoscalar nonet and predict non-negative scalar masses (in fact moderately high)—two nontrivial results. Current-algebra results are built in the tree graphs. If we employ smoothness assumptions, corrections to low-energy parameters can be expected to be small and indeed are found to be. These parameters include decay constants, wave-function renormalization constants, symmetry-breaking parameters, and scattering lengths. These quantities are very well determined by the one-loop approximation and there is good agreement with experiment where data are presently available.

Of the six parameters in the Lagrangian, five can be determined in terms of m_π, m_K, m_η, $m_{\eta'}$, and f_π, leaving one—m_σ—to be chosen to fit everything else, i.e., phase shifts. (For $l = 0, 1, 2$ there are 28 channels.) Within the limitations of our fit, we feel we have been successful in verifying the attractive idea that the pion decay constant, probed by the leptonic current, provides a good measure of the strength of the interactions nec-

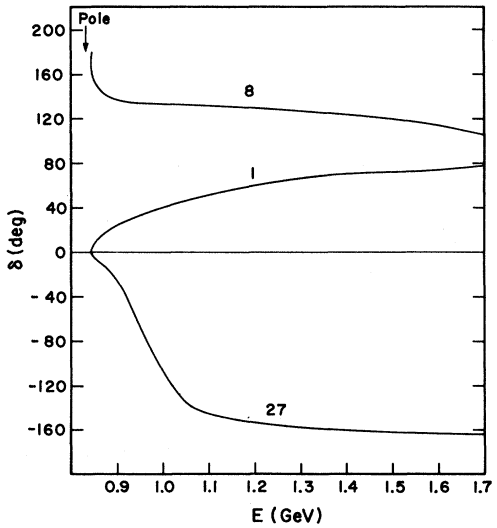

FIG. 8. S-wave phase shifts in the SU_3 limit corresponding to the parameters in Table VII.

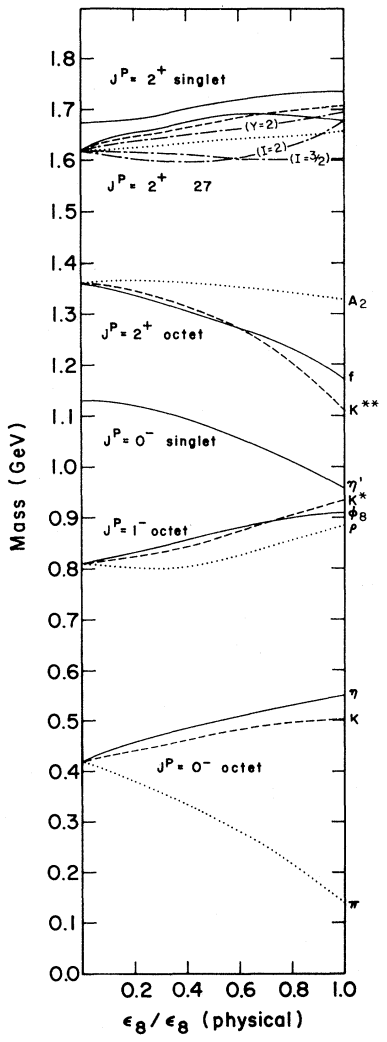

FIG. 9. Spectrum of states as a function of SU_3-symmetry breaking. The parameter ϵ_8 is in fact $C\epsilon_8 Z_{\epsilon_8}$, the full octet symmetry-breaking term in the Lagrangian. The masses of the scalar nonet are not given since they are poorly defined resonances (with the exception of the π_N).

essary to form resonances in purely strong-interaction processes.

It seems unlikely to us that all the shortcomings in the fit can be attributed to the approximation. The SU_3 $\underline{27}$ representation shows up with too much repulsion in S waves, and too much attraction in D waves, the former being more serious since we expect a higher reliability for S waves. We could not get the S^* effect in the $\pi\pi$ phase shift, but this is because our σ' is several hundred MeV too high. The κ is showing up too low. All these difficulties are tied to the fit at the tree order, and if a solution to these problems exists it can probably be discovered there.

While it is rather unlikely that such a simple model can account for the full dynamics in strong interaction, we have nonetheless demonstrated that a dynamical model encompassing those interesting theoretical features unified by Gell-Mann, Oakes, and Renner[9] can give a realistic dynamics beyond the low-energy region. In addition to providing a means to calculate correction in the low-energy region, this model can serve as a testing ground for some of the conjectures which have been accepted as reasonable but otherwise unchecked.[27]

The threshold dominance model[28] suggests that the nonanalytic behavior in the chiral symmetry limits can be used to isolate the leading corrections to low-energy theorems in a model-independent manner. Our perturbation calculation which does not require the expansion of the symmetry-breaking parameter ϵ and is correct to all order in ϵ can be used to test such an assumption. While the nonanalytic term may dominate at sufficiently small ϵ, at the physical point the analytic dependence in ϵ in the tree order cannot be ignored in comparison with the nonanalytic terms in the second order. Tables III and IV clearly demonstrate these effects. In addition, our calculation has a natural chiral-invariant cutoff mass from the scalar meson which is approximately half of the $2M_N$ used in Ref. 28. The meson form factor $f_+(0)$ is cutoff independent and has no ϵ_8 dependence in tree order. Our value $f_+(0) = 0.978$ agrees with the threshold dominance model.[29] The disagreement on other quantities such as f_K/f_π can be traced to the sizable contributions from the ϵ_8 term in the tree order together with the difference in the cutoff mass. Further study of this model may help to provide a better understanding of model-independent consequences of chiral symmetry.

ACKNOWLEDGMENT

One of us (R. H.) would like to express his appreciation for the hospitality extended to him by the Tulane University Physics Department, where some of the final phases of this work were completed.

APPENDIX A: SECOND-ORDER FEYNMAN GRAPHS

The box and triangle graphs were needed in this calculation for general values of all internal and external masses. However, none of the graphs needed in this calculation have anomalous thresholds. Hence they could be evaluated as dispersion integrals over the normal threshold discontinuity function. We have found a new form of this function for the general mass case which simplifies the evaluation of these graphs. In this appendix we give a procedure to evaluate the box graph and outline the steps to relate our discontinuity function to the form originally found by Mandelstam.[30]

1. Box graph

The variables defining the box graph $A(s, t, m_i^2, m_{ij}^2)$ are defined in Fig. 10. A is defined

$$A = i\int \frac{d^4k}{(2\pi)^4}\left(\prod_{i=1}^{4}\left[(q_i+k)^2 - m_i^2 + i\epsilon\right]\right)^{-1}. \quad \text{(A1)}$$

A is invariant under the replacement $q_i^\mu \to q_i^\mu + k^\mu$ for arbitrary k^μ. We use this freedom to put q_i on their respective internal mass shells. Our conventions are summarized as follows:

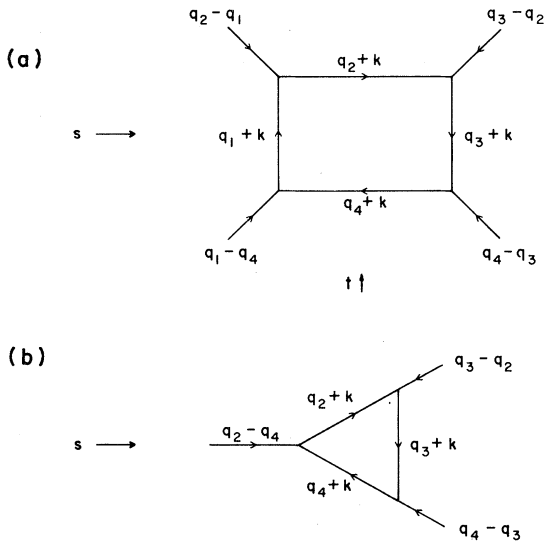

FIG. 10. Definition of variables for box and triangle graphs used in Appendix A.

$$q_i^2 = m_i^2 = (\text{internal mass})^2,$$

$$\text{external mass}^2 \equiv m_{ij}^2 = (q_i - q_j)^2 \qquad [(ij) = (12), (23), (34), (41)], \quad \text{(A2)}$$

$$s = (q_2 - q_4)^2 ,$$

$$t = (q_1 - q_3)^2 .$$

Define the matrix of invariants

$$Y_{ij} = -q_i \cdot q_j . \quad \text{(A3)}$$

The Y_{ij} are related to the variables (A2) as follows:

$$Y_{ii} = -m_i^2 ,$$

$$Y_{ij} = \tfrac{1}{2}(m_{ij}^2 - m_i^2 - m_j^2) \quad [(ij) = (12), (23), (34), (41)],$$

$$Y_{24} = \tfrac{1}{2}(s - m_2^2 - m_4^2) , \quad \text{(A4)}$$

$$Y_{13} = \tfrac{1}{2}(t - m_1^2 - m_3^2) .$$

Writing the box graph A in terms of the s-channel discontinuity A_s,

$$A(s,t) = \int_{(m_2+m_4)^2}^{\infty} \frac{ds'}{\pi} \frac{A_s(s',t)}{s'-s} , \quad \text{(A5)}$$

the discontinuity function can be written

$$A_s(s,t) = \frac{1}{64\pi(|Y|)^{1/2}} \ln \frac{|Y^{(1)}_{(3)}| + (-|Y^{(13)}_{(13)}||Y|)^{1/2}}{|Y^{(1)}_{(3)}| - (-|Y^{(13)}_{(13)}||Y|)^{1/2}} , \quad \text{(A6)}$$

where

$$|Y| = \det(Y) ,$$

$$|Y^{(1)}_{(3)}| = \det \begin{pmatrix} Y_{21} & Y_{22} & Y_{24} \\ Y_{31} & Y_{32} & Y_{34} \\ Y_{41} & Y_{42} & Y_{44} \end{pmatrix} , \quad \text{(A7)}$$

$$|Y^{(13)}_{(13)}| = \det \begin{pmatrix} Y_{22} & Y_{24} \\ Y_{24} & Y_{44} \end{pmatrix} .$$

The notation $|Y^{(ij\cdots)}_{(kl\cdots)}|$ means the determinant of the matrix obtained from Y by deleting the $(i,j\cdots)$ rows and $(k,l\cdots)$ columns of the matrix Y.

Considerable care is in order in evaluating (A5) and (A6) for general s, t, m_{ij}^2, and m_i^2 because of the complicated singularity structure of the box graph. The importance of the form (A6) lies in the fact that the singularity structure of the box graph has been analyzed in the literature[31] in terms of the variables that occur in Eq. (A6). To see this we make use of the following identity to eliminate $|Y^{(1)}_{(3)}|$:

$$|Y^{(1)}_{(3)}|^2 = |Y^{(1)}_{(1)}||Y^{(3)}_{(3)}| - |Y^{(13)}_{(13)}||Y| . \quad \text{(A8)}$$

The vanishing of these determinants that now occur give rise to singularities in the box graph and, in fact, have names[31]:

$|Y| = 0$ "box singularity,"

$|Y^{(i)}_{(i)}| = 0$ "triangle singularity,"

$|Y^{(ij)}_{(ij)}| = 0$ "normal threshold."

Figure 2.4.4 of Ref. 31 gives a plot of these singularities and is immensely useful in using Eq. (A6).

The derivation of (A6) is lengthy and will not be given here. Rather we will establish a correspondence between our form and that of Mandelstam.[30] The discontinuity formula is his Eq. (3.21). The correspondence is

$$|Y| = w^2 q_e^2 q_0^2 q_i^2 (z^2 + z_{ie}'^2 + z_{i0}'^2 - 1 - 2zz_{ie}'z_{i0}') ,$$

$$|Y^{(1)}_{(3)}| = w^2 q_e q_0 q_i^2 (z - z_{ie}' z_{i0}') , \quad \text{(A9)}$$

$$|Y^{(13)}_{(13)}| = -q_i^2 w^2 .$$

The right-hand sides of Eq. (A9) are the variables in the notation of Ref. 30. These identities may be easily established by making use of a trick used by Kibble.[32] Using the expressions for the determinants

$$\begin{vmatrix} p_1\cdot q_1 & \cdots & p_1\cdot q_4 \\ p_4\cdot q_1 & \cdots & p_4\cdot q_4 \end{vmatrix} = \frac{1}{24^2} \epsilon_{ijkl} p_i^{\alpha_1} p_j^{\alpha_2} p_k^{\alpha_3} p_l^{\alpha_4} \epsilon_{\alpha_1\alpha_2\alpha_3\alpha_4} \epsilon_{\beta_1\beta_2\beta_3\beta_4} q_a^{\beta_1} q_b^{\beta_2} q_c^{\beta_3} q_d^{\beta_4} \epsilon_{abcd}$$

and (A10)

$$\begin{vmatrix} p_1\cdot q_1 & \cdots & p_1\cdot q_3 \\ p_3\cdot q_1 & \cdots & p_3\cdot q_3 \end{vmatrix} = \frac{1}{6^2} \epsilon_{ijk} p_i^{\alpha_1} p_j^{\alpha_2} p_k^{\alpha_3} \epsilon_{\alpha_1\alpha_2\alpha_3\mu} \epsilon^{\mu}_{\beta_1\beta_2\beta_3} q_a^{\beta_1} q_b^{\beta_2} q_c^{\beta_3} \epsilon_{abc} ,$$

Equations (A9) are established by going to the s-channel c.m. frame and taking advantage of the invariance in these expressions under the replacement

$$P_i^{\mu} \to P_i^{\mu} + AP_j^{\mu} + BP_k^{\mu} + CP_l^{\mu} .$$

Plugging (A9) into (A6) gives Mandelstam's results up to a factor of 4. (The discrepancy is due to an error in Mandelstam's expression.)

2. Triangle graph

The triangle graph is a simple limit of the box graph which we give here. A more conventional

form for the triangle graph is given in Appendix B on partial-wave analyses for those readers who do not find this form transparent.

The triangle graph $T(s)$ defined by the variables in Fig. 10 is a simple limit of the box graph. The s discontinuity T_s is given in terms of A_s [Eq. (A6)] by the relation

$$T_s = -\lim_{m_1^2 \to \infty} (m_1^2 A_s) . \tag{A11}$$

In this limit

$$\begin{aligned} &|Y| \to \tfrac{1}{4} m_1^4 |Y'| , \\ &|Y^{(1)}_{(3)}| \to -\tfrac{1}{2} m_1^2 |Y'^{(1)}_{(3)}| , \\ &|Y^{(13)}_{(13)}| = |Y'^{(13)}_{(13)}| , \end{aligned} \tag{A12}$$

where

$$Y' = \begin{bmatrix} 0 & 1 & 1 & 1 \\ 1 & Y_{22} & Y_{23} & Y_{24} \\ 1 & Y_{32} & Y_{33} & Y_{34} \\ 1 & Y_{42} & Y_{43} & Y_{44} \end{bmatrix} . \tag{A13}$$

T itself can be evaluated through a dispersion integral over T_s as in Eq. (A5).

We also need the triangle graph in which one leg is a vector current. Choosing the (2, 4) leg for the current, we define

$$T^\mu = i \int \frac{d^4k}{(2\pi)^4} \frac{q_2^\mu + q_4^\mu + 2k^\mu}{\prod_{i=2}^4 [(q_i + k)^2 - m_i^2 + i\epsilon]} . \tag{A14}$$

The standard form factors are defined

$$T^\mu = (q_4 + q_2 - 2q_3)^\mu \, T_{(+)} + (q_4 - q_2)^\mu T_{(-)} . \tag{A15}$$

$T_{(+)}$ and $T_{(-)}$ also satisfy unsubtracted dispersion relations [Eq. (A5)]. We give their discontinuities $T_{(+)s}$, $T_{(-)s}$:

$$T_{(+)s} = -\frac{1}{|Y'|} \{ |Y'^{(1)}_{(3)}| T_s + \tfrac{1}{4} (-|Y^{(13)}_{(13)}|)^{1/2} \}; \tag{A16}$$

$T_{(-)s}$ is given through the relation

$$(m_4^2 - m_2^2) T_s = (m_{43}^2 - m_{23}^2) T_{(+)s} + s T_{(-)s} . \tag{A17}$$

The latter equations can be derived from Eq. (A14) by evaluating $(q_4 - q_2)_\mu T^\mu$ and taking the imaginary part.

APPENDIX B: PARTIAL-WAVE PROJECTIONS

The s-channel partial-wave projections are defined for the scattering $a + b \to c + d$ as

$$a_l(s) = \tfrac{1}{2} \int_{-1}^{+1} dz A(s, t) P_l(z) , \tag{B1}$$

where $z = \cos\theta$, θ being the scattering angle between a and c in the c.m. frame. Equation (B1) is converted to the Froissart-Gribov form by writing $A(s, t)$ as a fixed-s dispersion relation and performing the integration over z. We first evaluate Eq. (B1) for all the cases of interest in subsection 1, and then give the dispersion relations in subsection 2.

1. Pole terms

We need the partial-wave projections of pole terms in t for lowest-order graphs and from the dispersion denominators in second order.

For future reference we define the c.m. momentum

$$p(s, m_1^2, m_2^2) = \left[\frac{s^2 - 2s(m_1^2 + m_2^2) + (m_1^2 - m_2^2)^2}{4s} \right]^{1/2} \tag{B2}$$

and $z = \cos\theta$,

$$z(t, s, m_a^2, m_b^2, m_c^2, m_d^2) = \frac{\Lambda(t, s, m_a^2, m_b^2, m_c^2, m_d^2)}{p(s, m_a^2, m_b^2)\, p(s, m_c^2, m_d^2)} , \tag{B3}$$

$$\begin{aligned} &\Lambda(t, s, m_a^2, m_b^2, m_c^2, m_d^2) \\ &\quad = \tfrac{1}{2} [t - m_b^2 - m_d^2 \\ &\qquad + (1/2s)(s + m_b^2 - m_a^2)(s - m_d^2 - m_c^2)] . \end{aligned} \tag{B4}$$

For the purpose of these projections we shorten the notation to

$$\begin{aligned} p_i &= p(s, m_a^2, m_b^2) , \\ p_f &= p(s, m_c^2, m_d^2) , \\ z_t &= z(t, s, m_a^2, m_b^2, m_c^2, m_d^2) , \\ \Lambda_t &= \Lambda(t, s, m_a^2, m_b^2, m_c^2, m_d^2) , \\ z_t &= \Lambda_t / p_i p_f . \end{aligned} \tag{B5}$$

The basic integral needed is

$$\tfrac{1}{2} \int_{-1}^{+1} dz \, P_l(z) \frac{1}{\sigma^2 - t} \equiv \left[\frac{1}{\sigma^2 - t} \right]_l = \frac{1}{2 p_i p_f} Q_l(z_{\sigma 2}) . \tag{B6}$$

There are computational advantages in defining a new function

$$\Theta_l^{(0)}(z, \Lambda) = \frac{1}{2} \frac{1}{(p_i p_f)^{l+1}} Q_l(z) , \tag{B7a}$$

$$= \frac{1}{2} \frac{1}{\Lambda^{l+1}} [z^{l+1} Q_l(z)] . \tag{B7b}$$

For values of z of interest, z^2 is real. For real z^2, $\mathrm{Re}\Theta_l^{(0)}$ is even in z and $\mathrm{Im}\Theta_l^{(0)}$ is odd in z. We also need

$$\Theta_l^{(1)}(z, \Lambda) = \frac{1}{4} \frac{1}{(p_i p_f)^{l+2}} \frac{d}{dz} Q_l(z) . \tag{B8}$$

In summary,

$$\left[\frac{1}{\sigma^2-t}\right]_l = (p_i p_f)^l \Theta_l^{(0)}(z_{\sigma^2}, \Lambda_{\sigma^2}) ,$$
$$\left[\frac{1}{(\sigma^2-t)^2}\right]_l = -(p_i p_f)^l \Theta_l^{(1)}(z_{\sigma^2}, \Lambda_{\sigma^2}) . \quad \text{(B9)}$$

The other forms needed are related to these by partial fractions, which include

$$\left[\frac{1}{\sigma^2-t}\,\frac{1}{m^2-t}\right]_l ,$$
$$\left[\frac{1}{\sigma^2-t}\,\frac{1}{m^2-t}\,\frac{1}{n^2-t}\right]_l , \quad \text{(B10)}$$
$$\left[\frac{1}{\sigma^2-t}\,\frac{1}{(m^2-t)^2}\right]_l .$$

2. Dispersion relations

The groups of graphs indicated in Fig. 3 are treated individually below.

(a) The group labeled a_1 in Fig. 3 involves the bubble graph. This can be evaluated analytically as is done in Ref. 5, Appendix B. However, a dispersion form in t is needs for the s-channel partial-wave projections which we give here. Referring to Fig. 11 and Eq. (5.2) we have

$$\overline{B}(t; m_1^2, m_2^2) = B(t; m_1^2, m_2^2) - B_0(\nu^2) ,$$
$$\overline{B}(t; m_1^2, m_2^2) = \overline{B}(0; m_1^2, m_2^2) - \frac{1}{8\pi^2}\int_{(m_1+m_2)^2}^{\infty} dt' \left(\frac{1}{t'-t} - \frac{1}{t'}\right) \times \frac{p(t', m_1^2, m_2^2)}{\sqrt{t'}} , \quad \text{(B11)}$$

where

$$\overline{B}(0, m_1^2, m_2^2) = \frac{1}{16\pi^2}\left(\ln\frac{m_1 m_2}{\nu^2} - 1 - \frac{m_1^2+m_2^2}{m_1^2-m_2^2}\ln\frac{m_2}{m_1}\right) . \quad \text{(B12)}$$

The group a_3 in Fig. 3 involve the triangle graph $T(t)$. The dispersion relation for the triangle is given in Appendix A. We translate it into conventional variables here. Referring to the labels in Fig. 11, we find

$$T(t) = -\frac{1}{8\pi^2}\int_{(m_1+m_2)^2}^{\infty} dt' \frac{1}{(t'-t)t'}\frac{p}{\sqrt{t'}}\Theta_0^{(0)}(z, \Lambda) , \quad \text{(B13)}$$

where

$$p = p(t', m_1^2, m_2^2) ,$$
$$z = z(m_3^2, t', m_1^2, m_2^2, m_a^2, m_c^2) . \quad \text{(B14)}$$

The form factors for the triangle contributions to the vector current as defined in Appendix A are also given in this form:

$$T_{(+)}(t) = -\frac{1}{8\pi^2}\int_{(m_1+m_2)^2}^{\infty}\frac{dt'}{t'-t}\frac{p^3}{\sqrt{t'}}\Theta_1^{(0)}(z, \Lambda) , \quad \text{(B15)}$$

$$(m_c^2 - m_a^2)\,T_{(+)}(t) + t\,T_{(-)}(t) = (m_2^2 - m_1^2)\,T(t) + \overline{B}(m_a^2; m_1^2, m_3^2) - \overline{B}(m_c^2; m_2^2, m_3^2) , \quad \text{(B16)}$$

where $\overline{B}$ is the bubble graph of Eq. (B11).

The box graph as given in Appendix A is given here as a fixed-s dispersion relation,

$$A(s, t) = \int_{(m_1+m_3)^2}^{\infty}\frac{dt'}{\pi}\frac{A_t(s, t')}{t'-t} , \quad \text{(B17)}$$

$$A_t(s, t) = \frac{1}{64\pi|Y|^{1/2}}\ln\frac{|Y_{(4)}^{(2)}| + [-|Y_{(24)}^{(24)}||Y|]^{1/2}}{|Y_{(4)}^{(2)}| - [-|Y_{(24)}^{(24)}||Y|]^{1/2}} .$$

Note that the internal masses in Fig. 11 are labeled the same as Appendix A. The external mass labels correspond as follows:

$$(12) \to a, \quad (23) \to c, \quad (34) \to d, \quad (41) \to b .$$

(b) The group of graphs in Fig. 3(b) are simply obtained from group (a) in Fig. 3 by

$$a_l(s)|_{\text{group b}} = (-)^l a_l(s)|_{\text{group a}} . \quad \text{(B18)}$$

(c) The group in Fig. 3(c) are pure S-wave graphs.

(d) The final graph is shown in Fig. 3(d). The labels are given in Fig. 11 together with the same

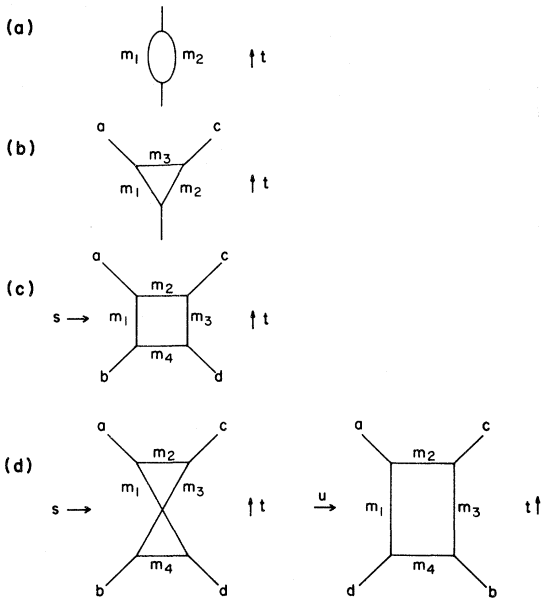

FIG. 11. Feynman graph labels used in Appendix B.

TABLE VIII. Block diagonalization of $P_8 \times P_8$ into Y, G, and I. For partial waves, the even (odd) exchange symmetry go with even (odd) l. For full amplitudes, they must be symmetrized or antisymmetrized in applying these forms. The matrices are symmetric.

Y	G	I	Symmetry	$\pi\pi$	$K\bar{K}$	$\eta\eta$
0	1	0	even	$\begin{matrix}\pi\pi \\ K\bar{K} \\ \eta\eta\end{matrix}\begin{pmatrix} 3A_{1111}-4A_{1212} & & \\ 2\sqrt{3}\,A_{1144} & 4A_{4466}+4A_{4657}+A_{4545} & \\ \sqrt{3}\,A_{1188} & 2A_{4488} & A_{8888}\end{pmatrix}$		
0	1	1	odd	$\begin{matrix}\pi\pi \\ K\bar{K}\end{matrix}\begin{pmatrix} 2A_{1212} & \\ 2\sqrt{2}\,A_{1245} & 2A_{4545}-2A_{4567}\end{pmatrix}$		
0	1	2	even	$\pi\pi(2A_{1212})$		
0	−1	0	odd	$K\bar{K}(2A_{4545}+2A_{4567})$		
0	−1	1	even	$\begin{matrix}\pi\eta \\ K\bar{K}\end{matrix}\begin{pmatrix} 2A_{1818} & \\ 2\sqrt{2}\,A_{1846} & 4A_{4657}+2A_{4545}\end{pmatrix}$		
0	−1	1	odd	$\pi\eta(2A_{1818})$		
1		$\frac{1}{2}$		$\begin{matrix}\pi K \\ \eta K\end{matrix}\begin{pmatrix} 2A_{1414}+4A_{1425} & \\ 2\sqrt{3}\,A_{3448} & 2A_{4848}\end{pmatrix}$		
1		$\frac{3}{2}$		$\pi K(2A_{1414}-2A_{1425})$		
2		0	odd	$KK(2A_{4747}-A_{4545}+2A_{4567})$		
2		1	even	$KK(2A_{4545})$		

graph in its planar form to aid in the identification of the variables Y_{ij}. The Y_{ij} are given in Eq. (A4) with the exception of Y_{24}, which is

$$Y_{24} = \tfrac{1}{2}(u - m_2^2 - m_4^2)\,, \qquad s+t+u = \Sigma \equiv m_a^2 + m_b^2 + m_c^2 + m_d^2\,. \tag{B19}$$

The external-mass labels of Appendix A correspond to the present labels as follows:

$$(12) \to a, \quad (23) \to c, \quad (34) \to b, \quad (41) \to d.$$

We need the box graph $A(u, t)$ as a fixed-s dispersion relation where we adhere to the convention that the first argument (u) is the variable with the (2, 4) intermediate state and the second variable (t) with the (1, 3) intermediate state:

$$A(u,t) = \int_{t_R}^{\infty} \frac{dt'}{\pi}\,\frac{A_t[u(t'),t']}{t'-t} - \int_{-\infty}^{t_L} \frac{dt'}{\pi}\,\frac{A_u[u(t'),t']}{t'-t}\,. \tag{B20}$$

The integrations are at fixed s; hence

$$u(t') = -t' - s + \Sigma\,, \qquad t_L = \Sigma - s - (m_2+m_4)^2\,, \qquad t_R = (m_1+m_3)^2\,. \tag{B21}$$

The discontinuities A_t and A_u are given by Eq. (B17) and Eq. (A6), respectively, with the understanding that Y_{24} is modified by Eq. (B19).

APPENDIX C: INTERNAL-SYMMETRY PROJECTIONS

The projection operators for diagonalizing the amplitudes into Y, I, and G parity and in the SU_3 limit in terms of SU_3 representations are given here.

(i) Y, I, G. The projection operators $P^{(Y,I,G)}_{ij;kl}$ are properly normalized:

$$P_{ij,kl}P_{kl,mn} = P_{ij,mn}\,.$$

$\pi_i\,\pi_j (i, j = 1, 2, 3)$:

$$P^{(0,0,+)}_{ij,i'j'} = \tfrac{1}{3}\delta_{ij}\delta_{i'j'}\,,$$

$$P^{(0,2,+)} = \tfrac{1}{2}(\delta_{ii'}\delta_{jj'} + \delta_{ij'}\delta_{ji'}) - P^{(0,0,+)}\,,$$

$$P^{(0,1,+)} = \tfrac{1}{2}\epsilon_{ijk}\epsilon_{i'j'k}\,.$$

$K_i K_j (i, j = 4, 5, 6, 7)$:

$$P^{(0,1,+)} = \sum_{k=1}^{3} d_{ijk}d_{i'j'k}\,,$$

$$P^{(0,0,+)} = \tfrac{1}{4}\delta_{ij}\delta_{i'j'}\,,$$

$$P^{(\pm 2,1)} = \tfrac{1}{2}(\delta_{ii'}\delta_{jj'} + \delta_{ij'}\delta_{ji'}) - P^{(0,1,+)} - P^{(0,0,+)} ,$$

$$P^{(0,1,+)} = \sum_{k=1}^{3} f_{ijk} f_{i'j'k} ,$$

$$P^{(0,0,-)} = \tfrac{1}{3} f_{ij8} f_{i'j'8} ,$$

$$P^{(\pm 2,1)} = \tfrac{1}{2}(\delta_{ii'}\delta_{jj'} - \delta_{ij'}\delta_{ji'}) - P^{(0,0,-)} - P^{(0,1,+)} .$$

$\pi_i K_j$ $(i = 1, \ldots, 3;\ j = 4, \ldots, 7)$:

$$P^{(\pm 1,1/2)} = \tfrac{4}{3} \sum_{k=1}^{4} d_{ijk} d_{i'j'k} ,$$

$$P^{(\pm 1,3/2)} = \delta_{ii'}\delta_{jj'} - P^{(\pm 1,1/2)} .$$

For elastic scattering, the diagonalized amplitudes can be found from

$$A_{ijkl} = \sum_{IYG} A^{(Y,I,G)} P^{(Y,I,G)}_{ijkl} .$$

The A_{ijkl} must be symmetrized as antisymmetrized—for partial waves, this is automatic. For $\pi_i \pi_j K_k K_l$ we can use the tensors (not projection operators)

$$T^{(0,0,+)}_{ij,i'j'} = \frac{1}{2\sqrt{3}} \delta_{ij}\delta_{i'j'} ,$$

$$T^{(0,1,+)} = \frac{1}{\sqrt{2}} \epsilon_{ijk}\epsilon_{i'j'k} .$$

The expansion tensors involving η are easily written down. Table VIII gives the diagonalized amplitudes expressed in terms of the A_{ijkl}.

(ii) SU_3 limit. These operators, normalized as above, are

$$P^{1}_{ij,i'j'} = \tfrac{1}{8}\delta_{ij}\delta_{i'j'} ,$$

$$P^{8s} = \tfrac{3}{5} \sum_{k=1}^{8} d_{ijk} d_{i'j'k} ,$$

$$P^{27} = \tfrac{1}{2}(\delta_{ii'}\delta_{jj'} + \delta_{ij'}\delta_{ji'}) - P^{1} - P^{8s} ,$$

$$P^{8a} = \tfrac{1}{3} \sum_{k=1}^{8} f_{ijk} f_{i'j'k} ,$$

$$P^{(10+\overline{10})} = \tfrac{1}{2}(\delta_{ii'}\delta_{jj'} - \delta_{ij'}\delta_{ji'}) - P^{8a} .$$

---

*Work supported in part by the LSU Council on Research Summer Fellowship.

[1] J. Schwinger, Ann. Phys. (N.Y.) 2, 407 (1957); M. Gell-Mann and M. Lévy, Nuovo Cimento 16, 705 (1960); M. Lévy, *ibid.* 52, 23 (1967).

[2] S. Gasiorowicz and D. Geffen, Rev. Mod. Phys. 41, 531 (1969).

[3] J. L. Basdevant and B. W. Lee, Phys. Rev. D 2, 1680 (1970); R. Olshansky, *ibid.* 4, 2440 (1971); P. Carruthers and R. W. Haymaker, *ibid.* 4, 1808 (1971); 6, 1528 (1972); D. W. McKay and W. F. Palmer, *ibid.* 5, 856 (1972); D. W. McKay, W. F. Palmer, and R. F. Sarraga, *ibid.* 8, 2532 (1973); K. S. Jhung and R. S. Willey, *ibid.* 9, 3132 (1974); J. J. Brehm, *ibid.* 9, 1818 (1974).

[4] J. Schechter and Y. Ueda, Phys. Rev. D 3, 2874 (1971).

[5] L.-H. Chan and R. W. Haymaker, Phys. Rev. D 7, 415 (1973).

[6] B. W. Lee, Nucl. Phys. B9, 649 (1969).

[7] K. Symanzik, Commun. Math. Phys. 16, 48 (1970).

[8] L.-H. Chan and R. W. Haymaker, Phys. Rev. D 7, 402 (1973). Referred to as paper I.

[9] M. Gell-Mann, R. J. Oakes, and B. Renner, Phys. Rev. 175, 2195 (1968).

[10] S. L. Adler, Phys. Rev. 137, B1022 (1965).

[11] J. Zinn-Justin, Phys. Rep. 1C, 55 (1971).

[12] We use standard definitions of λ^i, f_{ijk}, and d_{ijk} as given in Ref. 2.

[13] In the formalism that follows, C is a frill, introduced for generality, and it can be set equal to 1. It is introduced to renormalize an unphysical quantity which is described below, and is useful for studying chiral limits but is not essential. For the reader who wishes to get an idea of our renormalization approach and avoid details see our following paper [L.-H. Chan and R. W. Haymaker, Phys. Rev. D 10, 4170 (1974)] on the SU_2 σ model that parallels this one.

[14] S. Coleman, J. Wess, and B. Zumino, Phys. Rev. 177, 2239 (1969).

[15] We take pains to separate tree- and second-order parts of all quantities in this paper. However, in this section, we are dealing with exact results, and quantities such as f_{ia} are full physical quantities.

[16] L. M. Chounet, J.-M. Gaillard, and M. K. Gaillard, Phys. Rep. 4C, 199 (1972).

[17] M. Ademollo and R. Gatto, Phys. Rev. Lett. 13, 264 (1964).

[18] S. Weinberg, Phys. Rev. Lett. 17, 616 (1966).

[19] S. D. Protopopescu *et al.*, Phys. Rev. D 7, 1279 (1973).

[20] B. Hyams *et al.*, Nucl. Phys. B64, 134 (1973).

[21] There is a calculation covering a similar scope as this calculation based on unrenormalizable Yang-Mills fields: D. Iagolnitzer, J. Zinn-Justin, and J. B. Zuber, Nucl. Phys. B60, 233 (1973). They were able to get the S^* effect by varying a subtraction constant. This is what we did to move the σ'—we freed Z_{f_1} from its renormalization condition. They have independent subtraction terms in each channel in the S wave. In our calculation there is no such freedom since everything is well defined, and changing Z_{f_1} changes all the partial waves. With freedom in subtraction constants in each S-wave channel we could get a far better fit. They have suggested a renormalizable version of their model and we feel that that version should be compared to this calculation to assess the merits of one approach over the other.

[22] D. Cohen *et al.*, Phys. Rev. D 7, 661 (1973).

[23] N. B. Darusoy *et al.*, Phys. Lett. 45B, 517 (1973).

[24] G. C. Fox and M. L. Griss, Nucl. Phys. B80, 403 (1974).

[25] R. Mercer *et al.*, Nucl. Phys. B32, 381 (1971).

[26]This choice was motivated by holding $\mathcal{L}_{sym}$ fixed in going to the SU_3 limit.
[27]R. Dashen, Phys. Rev. 183, 1245 (1969); R. Dashen and M. Weinstein, *ibid.* 183, 1291 (1969).
[28]L. F. Li and H. Pagels, Phys. Rev. Lett. 26, 1204 (1971); Phys. Rev. D 5, 1509 (1972); Phys. Rev. Lett. 27, 1089 (1971); P. Langacker and H. Pagels, *ibid.* 30, 630 (1973); Phys. Rev. D 8, 4595 (1973); 10, 2904 (1974).
[29]S. Wada, Phys. Lett. 49B, 175 (1974).
[30]S. Mandelstam, Phys. Rev. 115, 1741 (1959).
[31]R. J. Eden, P. V. Landshoff, D. I. Olive, and J. C. Polkinghorne, *The Analytic S-Matrix* (Cambridge Univ. Press, Cambridge, 1966).
[32]T. W. B. Kibble, Phys. Rev. 117, 1159 (1960).

PHYSICAL REVIEW D VOLUME 10, NUMBER 12 15 DECEMBER 1974

π-π scattering in the SU_2 σ model

Lai-Him Chan and Richard W. Haymaker*
Department of Physics and Astronomy, Louisiana State University, Baton Rouge, Louisiana 70803
(Received 15 July 1974)

We explore the freedom of choosing subtraction points in the renormalizable σ model of $\vec{\pi}$ and σ. Phase shifts are computed from Padé approximants in the one-loop approximation. Comparisons are made with a previous calculation and an SU_3 σ-model calculation. The phase of the scalar form factor of the pion is presented.

I. INTRODUCTION

In the preceding paper[1] (referred to as paper II) we described a calculation of phase shifts for the SU_3 σ model in the one-loop approximation. In this paper we do the same for a much simpler model—the SU_2 σ model.[2] Since a similar calculation has been done before by Basdevant and Lee[3] (referred to as BL) we need to justify doing it again. This paper differs from BL in the manner by which finite parts of renormalization counterterms are chosen. We describe a freedom in the renormalization procedure that is not discussed in BL. We advocate adopting a procedure in which perturbation theory is a power series in a physical quantity with a known value—in this case $1/f_\pi{}^2$—and in which all subtractions are at physically measurable quantities. The procedure in this paper is the direct analog of that in our paper II. Hence, in addition to exploring the renormalization freedom, this paper gives a direct comparison between these two models treated on the same footing and in the light of up-to-date phase-shift data that is substantially different from that used in Ref. 3.

The freedom we refer to can best be described by considering the hypothetical situation in which the σ particle is stable. Then a very natural renormalization procedure suggests itself. Since there are three parameters in the model, three quantities can be chosen to be fixed constants to all orders in perturbation theory—a natural set being m_π, m_σ, and the perturbation expansion parameter, which for us is in $1/f_\pi{}^2$, for BL in $1/\langle\sigma\rangle^2$ ($\langle\sigma\rangle$ = vacuum expectation value of the σ field). The statement that the expansion parameter has no higher-order corrections is a tautology, but there is a choice involved in what that parameter shall be. Renormalizing at the pion mass is a deep-seated prejudice based on the fact that we know the mass very well. If one knew instead the 10th derivative of a form factor very well, one could make a case of renormalizing at the physical quantity. Now, since the σ is in fact unstable and very wide, even if we were committed to renormalizing at its mass, there are a myriad of possible conditions one could think of to replace the strict mass renormalization condition for the stable σ.

Neither BL nor we are committed to renormalizing at the σ mass, although one of our renormalization prescriptions discussed here is in that spirit. This method (referred to as method II) is to demand that $d\delta_0^0/ds$ be a maximum at the tree value of the σ mass, where δ_0^0 is the $I=0$, $l=0$ $\pi\pi$ phase shift. A second method is given which exactly parallels our paper II (method I), in which the $I=0$, $l=0$ $\pi\pi$ amplitude is renormalized such that there are no second-order corrections at a low-energy on-mass-shell point. A consequence of both these methods is that as $f_\pi \to \infty$, with tree masses fixed, the ratio of (second order)/(tree) for all quantities goes to zero, all dynamically generated states go away, and the scalar resonances approach their zero-width approximations.